NAVAL POSTGRADUATE SCHOOL
Monterey, California

THESIS

INFLUENCE OF IGNITION ENERGY, IGNITION LOCATION, AND STOICHIOMETRY ON THE DEFLAGRATION-TO-DETONATION DISTANCE IN A PULSE DETONATION ENGINE

by

John P. Robinson III

June 2000

Thesis Advisor: Christopher M. Brophy
Co-Advisor: Tom J. Hofler

Approved for public release; distribution is unlimited.

REPORT DOCUMENTATION PAGE

Form Approved
OMB No. 0704-0188

1. AGENCY USE ONLY *(Leave blank)*	2. REPORT DATE	3. REPORT TYPE AND DATES COVERED
	June 2000	Master's Thesis

4. TITLE AND SUBTITLE
Influence Of Ignition Energy, Ignition Location, And Stoichiometry On The Deflagration-To-Detonation Distance In A Pulse Detonation Engine

5. FUNDING NUMBERS
Contract Number
N0001498WR20018

6. AUTHOR(S)
Robinson, John P. III

7. PERFORMING ORGANIZATION NAME(S) AND ADDRESS(ES)
Naval Postgraduate School
Monterey, CA 93943-5000

8. PERFORMING ORGANIZATION REPORT NUMBER

9. SPONSORING / MONITORING AGENCY NAME(S) AND ADDRESS(ES)
Office of Naval Research
Ballston Tower One
800 N. Quincy Street
Arlington, VA 22217-5600

10. SPONSORING / MONITORING AGENCY REPORT NUMBER

11. SUPPLEMENTARY NOTES
The views expressed in this thesis are those of the author and do not reflect the official policy or position of the Department of Defense or the U.S. Government.

12a. DISTRIBUTION / AVAILABILITY STATEMENT
Approved for public release; distribution unlimited.

12b. DISTRIBUTION CODE

13. ABSTRACT *(maximum 200 words)*

The feasibility of utilizing detonations for air-breathing propulsion is the subject of a significant research effort headed by the Office of Naval Research. Pulse Detonation Engines (PDE) have a theoretically greater efficiency than current combustion cycles. However, pulse detonation technology must mature beginning with research in the fundamental process of developing a detonation wave. This thesis explores various ignition conditions which minimize the deflagration-to-detonation transition distance (X_{DDT}) of a single detonation wave in a gaseous mixture.

Specifically, the minimum X_{DDT} was determined for different Ethylene and Oxygen/Nitrogen gaseous mixtures under varying ignition energy (0.33-8.31 Joules), mixture equivalence ratios (0.6-2.0), and ignitor locations. To conduct the experiments a 6ft. long, 3in. diameter tube combustor, support equipment, and operating software was built. Four independent test scenarios were investigated and trends developed to determine the minimum X_{DDT} while reducing oxidizer blend ratios.

Results show that X_{DDT} significantly depends on mixture equivalence ratio (φ) and was minimized at $\varphi \approx 1.1$. No dependence on ignition energies greater than 0.5 Joules was observed. A further reduction in X_{DDT} was observed with the ignitor located one combustor diameter from the head wall. These results will be useful in future designs of pre-detonators for larger PDEs.

14. SUBJECT TERMS
Detonation, Pulse Detonation Engine, Deflagration-to-Detonation Transition, DDT

15. NUMBER OF PAGES
94

16. PRICE CODE

17. SECURITY CLASSIFICATION OF REPORT	18. SECURITY CLASSIFICATION OF THIS PAGE	19. SECURITY CLASSIFI- CATION OF ABSTRACT	20. LIMITATION OF ABSTRACT
Unclassified	Unclassified	Unclassified	UL

NSN 7540-01-280-5500

Standard Form 298 (Rev. -89)
Prescribed by ANSI Std. 239-18

THIS PAGE INTENTIONALLY LEFT BLANK

Approved for public release; distribution is unlimited

INFLUENCE OF IGNITION ENERGY, IGNITION LOCATION, AND STOICHIOMETRY ON THE DEFLAGRATION-TO-DETONATION DISTANCE IN A PULSE DETONATION ENGINE

John P. Robinson III
Lieutenant, United States Navy
B.S., United States Naval Academy, 1993

Submitted in partial fulfillment of the
requirements for the degree of

MASTER OF SCIENCE IN APPLIED PHYSICS

from the

NAVAL POSTGRADUATE SCHOOL
June 2000

Author: _____
John P. Robinson III

Approved by: _____
Christopher M. Brophy, Thesis Advisor

_____
Tom J. Hofler, Co-Advisor

_____
William B. Maier II, Chairman
Department of Physics

THIS PAGE INTENTIONALLY LEFT BLANK

ABSTRACT

The feasibility of utilizing detonations for air-breathing propulsion is the subject of a significant research effort headed by the Office of Naval Research. Pulse Detonation Engines (PDE) have a theoretically greater efficiency than current combustion cycles. However, pulse detonation technology must mature beginning with research in the fundamental process of developing a detonation wave. This thesis explores various ignition conditions which minimize the deflagration-to-detonation transition distance (X_{DDT}) of a single detonation wave in a gaseous mixture.

Specifically, the minimum X_{DDT} was determined for different Ethylene and Oxygen/Nitrogen gaseous mixtures under varying ignition energy (0.33-8.31 Joules), mixture equivalence ratios (0.6-2.0), and ignitor locations. To conduct the experiments a 6ft. long, 3in. diameter tube combustor, support equipment, and operating software was built. Four independent test scenarios were investigated and trends developed to determine the minimum X_{DDT} while reducing oxidizer blend ratios.

Results show that X_{DDT} significantly depends on mixture equivalence ratio (φ) and was minimized at $\varphi \approx 1.1$. No dependence on ignition energies greater than 0.5 Joules was observed. A further reduction in X_{DDT} was observed with the ignitor located one combustor diameter from the head wall. These results will be useful in future designs of pre-detonators for larger PDEs.

THIS PAGE INTENTIONALLY LEFT BLANK

TABLE OF CONTENTS

LIST OF FIGURES

THIS PAGE INTENTIONALLY LEFT BLANK

LIST OF TABLES

THIS PAGE INTENTIONALLY LEFT BLANK

LIST OF ABBREVIATIONS and SYMBOLS

C_p	Constant Pressure Specific Heat
C-J	Chapman Jouget Point
c	Local Sonic Velocity
e	Total Internal Energy per Unit Mass
h	Enthalpy per Unit Mass
h^o	Specific Enthalpy
M	Mach Number
$\dot{m}$	Mass Flow Rate
p	Pressure
p_0	Ambient Pressure
p_{ref}	Reference Pressure
q	Total Heat Addition per Unit Mass
q_{cond}	Heat Addition per Unit Mass by Conduction
$q_{addition}$	Heat Addition by Combustion
$q_{1\to2}$	Heat Addition by Combustion
$q_{4\to0}$	Heat Released into Atmosphere
R	Specific Gas Constant
s	Entropy
T	Temperature
T_{ref}	Reference Temperature
u	Velocity
u'	Internal Energy
V_{det}	Detonation Velocity
W_{net}	Net Work
x	Position
X_{DDT}	Deflagration to Detonation Transition Distance
γ	Specific Heat Ratio
λ	Thermal Conductivity
η_{TH}	Thermal Efficiency
φ	Equivalence Ratio
ρ	Density
μ	Sensible Heat
ν	Specific Volume ($1/\rho$)

subscripts:

0	Ambient State
1	Pre-combustion State
2	Post-combustion State
3	Post-expansion State
4	Cycle End State

THIS PAGE INTENTIONALLY LEFT BLANK

I. INTRODUCTION

A. BACKGROUND

Almost all current propulsion systems utilize a constant pressure (C_p) combustion process to add energy to the working fluid. Most engine designs are based on the constant pressure burning of the fuel within the combustor. An approach, though not new, is emerging to investigate engine efficiency limits within the combustion process itself. This idea is based on the fact that fuels burn significantly more efficiently in a nearly constant volume compression based event verses a constant pressure process. In a practical flowing system, this is commonly referred to as a detonation. The practicality of applying a detonation to a propulsion system lies in the ability to couple this increase in thermal efficiency to an increase in propulsive efficiency. To do this, the physics behind establishing a detonation and its propagation along a combustor axis must be understood and harnessed before it can be used effectively in a controlled manner for propulsion applications.

B. HISTORY OF DETONATION RESEARCH

1. Discovery of the Detonation

The first recognized detonation, then called a 'violent explosion', was discovered and later patented by A. Nobel in 1863. He, with his father, invented a mercury fulminate ignitor that initiated a detonation in a nitroglycerine charge. He later perfected this process in 1867 with the significant invention of dynamite [Ref. 1], however the scientific understanding of the physics behind the detonation phenomena was lacking and required substantial research to develop the technology to the level existing today.

In the early 1870's, researchers such as F. A. Abel and M. Berthelot began to relate the strength of an explosion to how it was initiated and its propagation velocity. It was hypothesized that some form of mechanical or vibrational shock waves must initiate the detonation and that this wave must be sustained throughout the event. M. Berthelot and P. Vieille furthered this idea by analyzing the first measurements of detonation wave velocity conducted by F. A. Abel in 1874. The results were substantiated in similar experiments in the early 1880's. Bethelot and Vieille concluded, based on numerous tests of different fuels and oxidizers at different equivalence ratios, that the detonation velocity is uniform and only dependent on the fuel and its mixture ratios. [Ref. 1]

E. Mallard and H. Le Chatelier found another significant property of the detonation phenomenon in 1883. Using a new device called a drum-camera, they were able to demonstrate that a deflagration, under the right conditions, will transition into a detonation wave. This new information led to their experimental proof that the detonation process can be seen as a rapid adiabatic process whose energy drives the detonation wave. It was also noted that the detonation wave velocity was on the same order as the sound velocity of the products of the combustion. This led to the formulation that there is an inherent relation between the chemistry of the reactants, the conditions in which they are ignited, and the detonation properties they exhibit. [Ref. 1]

2. Formulation of the Chapman-Jouget Theory

The early discoveries and ideas produced in the 1880's led to several of the top thermodynamicists and chemists of the day to become interested in the new detonation phenomenon. In 1890, V. A. Michelson, working through the Rankine Theory, showed the detonation pressure as a function of the detonation velocity and the reactant's heat of

reaction, and that through the system of equations there are two possible solutions. This is the first insight in that reactants, at different conditions, will burn naturally around two distinct conditions. He also noted that there exists a convergence of pressures at the upper point, which correlated to the detonation process. This was later proven by the work of D. L. Chapman and E. Jouget. [Ref. 1]

Chapman-Jouget theory was recognized as the relationship between velocities of combustion wave processes and the pressures at which they occur. It also is the realization that there are two regions at which a combustion process may occur. The theory is named for two individuals who worked independently and demonstrated two distinct properties for combustion events. D. L. Chapman published his findings in 1899 that stated there exists a minimum velocity in which a detonation can occur and it is thermodynamically tied to the properties of the burned gas. The second part of the theory was provided by the work of E. Jouget. He worked from 1901-1905 and established the relation that the detonation wave velocity is equal to the sound velocity of the burned gas in which it propagated. He verified this result by comparing computed results with experimental data found by several of his predecessors. J. L. Crussard validated the C-J theory in 1907 by relating the two specific combustion pressure points on the Hugoniot curve (pressure-specific volume adiabat). The two solutions of the C-J theory can be seen on the well-publicized graph shown in Figure [1-1]. The upper C-J point is related to a detonation and the lower C-J point showing the deflagration region. [Ref. 1] The relationship of the Chapman-Jouget points with the Hugoniot curve and a description of the distinct solution regions will be looked at in detail in Chapter II. Research continued into the twentieth century as Von Neumann, Doring and Zeldovich further modeled the

detonation wave as a shock wave followed closely by the combustion process of the reactants.

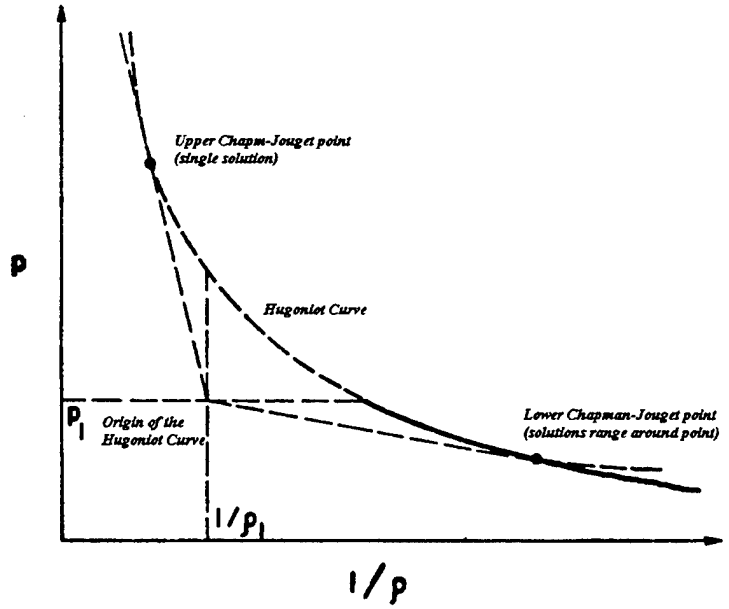

Figure [1-1]. Chapman-Jouget Solutions on the Hugoniot Curve. [From Ref. 2]

3. Past Applications of Detonations

With the physics of the detonation wave explained using C-J theory, many applications could be modeled and utilize the energy release rate of detonations. Before the 1890's, detonations were commonly used in explosions, fireworks, and in dynamite. However, in these applications the detonation was not controlled or readily understood. The first unsuccessful attempt to utilize the thermal efficiency of a detonation in a propulsion system was seen in the German's "Buzz Bombs" that created havoc among the Allied cities in World War II. Another attempt at applying pulsed combustion in a propulsion system occurred in the mid twentieth century in the United States under "Project Squid". This program studied the application of pulsed engines in both military and civilian combustion engines. These pulsejet engines were shown not to be detonation engines since their combustion processes occurred with a subsonic flame speed in a

"tuned-port" combustion chamber. These efforts were later abandoned since it was determined that the propulsion system did not have a high overall efficiency. [Ref. 3]

C. CURRENT DETONATION RESEARCH

There is a lot of promising research in detonation fundamentals and applications by government labs, commercial enterprises, and academic facilities. The concept of utilizing detonations for propulsion was renewed in the 1960's with propulsion concept studies for new high-speed unmanned vehicles. Since that time, there have been many studies, experiments and simulations run by several independent organizations. The most documented and perhaps most well known of these studies include the research of Adroit Systems Incorporated and the Office of Naval Research funded academic consortium. Each of these independent groups has aggressive test plans in hopes to gain insight in the intricacies of effectively creating and controlling detonations for a useful propulsion system design.

Adroit Systems Incorporated (ASI) has taken a vocal lead in the commercial development of detonation technology. T. Bussing and G. Pappas of ASI published a technical paper for the American Institute of Aeronautics and Astronautics conference in January 1994 that summarized the technical feasibility of designing and building a Pulse Detonation Engine (PDE). This paper outlined some basic physics of detonations and arguments supporting future research and development of a PDE [Ref. 4]. Since that time ASI has developed and patented many pulse detonation technologies, such as using multiple combustors with a rotary valve. They have also invested in a Pulse Detonation Rocket Engine (PDRE) concept and using detonations for material synthesis and intense sound level generation [Ref. 5].

The United States Department of Defense is investigating detonation technology for use in future high-speed missile and aircraft propulsion systems or as a non-lethal weapon. The Office of Naval Research (ONR) has organized an integrated research team in hopes to understand the requirements needed for PDE development. This team consists of six prominent university laboratories and the Navy's research facilities including the Naval Research Laboratory (NRL), Naval Postgraduate School (NPS) and the Naval Air Warfare Center (NAWC). The combined work of these institutions will cover PDE research from fundamental detonation studies to multi-cycle operation and cycle analysis. Figure [1-2] is a slide outlining the detonation research roadmap and the responsibilities of the participating institutions.

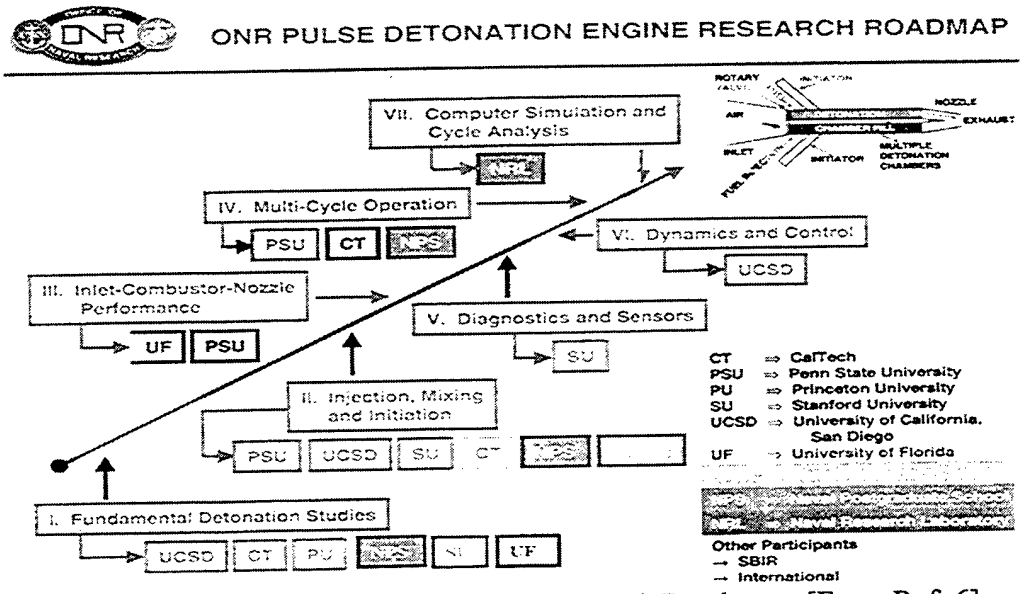

Figure [1-2]. ONR Pulse Detonation Research Roadmap. [From Ref. 6]

This thesis will explore some of the topics NPS is tasked to research in part one of this roadmap. Specifically, it researches the ignition energy/power requirements for minimization of X_{DDT} as a function of ignition location and equivalence ratio for an ethylene and oxygen fuel mixture. [Ref. 6]

II. PHYSICS OF A DETONATION WAVE

A. INTRODUCTION

In order to begin a detailed analysis of detonation waves, one must first look into the subject of combustion. Combustion is defined as an exothermic chemical reaction between a fuel and an oxidizer that once initiated can sustain itself as long as the ingredients in the proper proportions are present. However, not all combustion events are the same. The velocity at which a combustion wave propagates through a mixture is an accurate measure of the strength or violence of the event. This velocity is dependent on several factors including the mixture composition, pressure, temperature, and the geometry of the volume where the combustion occurs. The following sections describe three distinct combustion events and how they are initiated, sustained, and terminated.

B. DEFINITIONS

1. Deflagration

Deflagration is the combustion process most commonly utilized in current flight propulsion systems such as ramjets, turbojets and rocket engines. Some practical examples of this type of combustion include a burning match, a campfire, or a flame moving along an open gasoline spill. A closer look reveals that a deflagration is a combustion wave propagating at a subsonic speed. The deflagration flame speed is a function of pressure, temperature, and turbulence of the reactants, and the permittable range is correctly predicted by the C-J theory falling somewhere near the lower C-J point. This speed is heavily dependent on the chemical makeup, mass diffusion rates and thermal transfer rates of the reactants. Typical wave speeds for a deflagration

combustion wave range from 1-30$^{m}/_{s}$. Though deflagration is the most common and most utilized combustion process, it is theoretically not the most efficient thermodynamic path for combustion to occur. This is because the entropy of the resulting gases is maximized, which reduces the amount of work available. [Ref. 2]

2. Explosion

An explosion can be a combustion or non-combustion event and occurs when a reaction releases energy at a much greater rate than the surrounding environment can absorb. This exothermic reaction rate increases exponentially with the subsequent increase in temperature and pressure. This causes the combustion event to go quickly out of control. The volume of the explosion will expand due to the increase of pressure and break any boundaries placed on it. Even though the explosion is powerful and occurs very fast, the combustion event itself occurs as a deflagration wave as it travels through unburned reactants. This becomes an important distinction between the explosion and the detonation wave. [Ref. 3]

3. Detonation

A detonation is a combustion event that happens when special conditions exist. It can be described as a supersonic combustion event that propagates at high velocities and produces a violent and rapid combustion of the reactants due to the strong shock wave leading the detonation. The mechanics of the detonation will be derived and discussed in detail in Section C of this chapter.

A qualitative distinction between detonations and deflagrations is a good format to view the extreme differences between the two. The reference frame for this analysis will be a one-dimensional stationary combustion wave. The properties used to describe

the event will include ratios of, reactant velocity (u), sonic velocity (c), density (ρ), temperature (T) and pressure (p). Subscripts will delineate the burned and unburned side of the wave. Figure [2-1] is a schematic diagram of the reference frame used for the analysis.

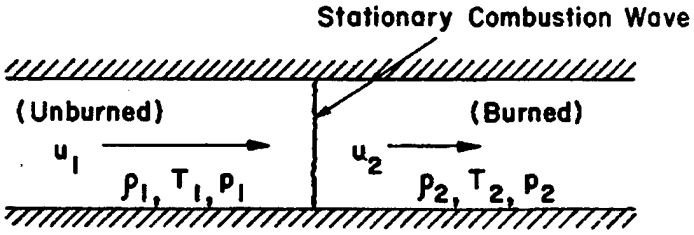

Figure [2-1]. Schematic of Stationary 1-D Combustion Wave. [From Ref. 2]

A qualitative comparison between a deflagration and detonation is given in Table [2-1]. Note that the detonation pressures, velocities and density ratios are significantly larger than the deflagration process. These results depict dramatic differences between the two combustion events and lead to questions as to how it happens, and what can be gained from it.

Table [2-1]. Qualitative Difference Between Detonation and Deflagration. [From Ref. 2]

Properties	Deflagration	Detonation
u_1/c_1	0.0001 - 0.03	5 – 10
u_2/u_1	4 - 6 (acceleration)	0.4 - 0.7 (deceleration)
p_2/p_1	≅ 0.98 (slight expansion)	13 - 55 (compression)
T_2/T_1	4 - 16 (heat addition)	8 - 21 (heat addition)
ρ_2/ρ_1	0.06 - 0.25	1.7 - 2.6

C. DETONATION WAVE THEORY

1. Thermodynamics of a Detonation Wave

Any detailed study into the origins and properties of a detonation wave must begin with a derivation and analysis of the Hugoniot curve. This relationship between enthalpy (h), pressure, and density of the gases in a combustion event is directly related

to the various combustion conditions. The Chapman-Jouget points discussed in Chapter 1 are the two physical solutions to the Hugoniot relation for the constant area geometry given, and will the basis for analyzing the detonation phenomena.

The governing equations of a thermodynamic process must be derived from the basic conservation equations of physics. These equations are:

Continuity equation: $$\frac{d(\rho u)}{dx} = 0 \qquad [2\text{-}1]$$

Conservation of momentum: $$\rho u \frac{du}{dx} + u \frac{d(\rho u)}{dx} = -\frac{dp}{dx} \qquad [2\text{-}2]$$

Conservation of energy: $$\rho u \left[\frac{d}{dx} \left(h + \frac{u^2}{2} \right) \right] = -\frac{d}{dx}(q_{cond}) \qquad [2\text{-}3]$$

Where the enthalpy (h) and the heat added (q_{cond}) to the system is defined by

$$h = C_p T + h^\circ \qquad [2\text{-}4]$$

$$q = h_1^\circ - h_2^\circ \qquad [2\text{-}5]$$

$$q_{cond} = -\lambda \frac{dT}{dx} \qquad [2\text{-}6]$$

This derivation assumes steady one-dimensional flow, with no external heat added or rejected, negligible interdiffusion effects, no viscous effects, and occurs within a constant area combustor. By analyzing the detonation in this form, it can be viewed as a supersonic shock wave with calculable properties in front of and behind the wave. By integrating equation [2-1] the concept of a constant mass flow rate ($\dot{m}$) is revealed by

$$\int d(\rho u) = \int 0 dx \Rightarrow \rho u = const. = \dot{m} \qquad [2\text{-}7]$$

Substituting equation [2-1] into the momentum equation and simplifying, equation [2-2] becomes

$$\frac{d}{dx}\left[\rho u^2 + p\right] = 0 \qquad [2\text{-}8]$$

Integrating equation [2-8] gives an alternate momentum equation to work with.

$$\rho u^2 + p = const.' \qquad [2\text{-}9]$$

By similar analysis, the energy equation [2-3] becomes

$$\rho u\left(C_p T + h^\circ + \frac{u^2}{2}\right) - \lambda\frac{dT}{dx} = const.'' \qquad [2\text{-}10]$$

Referring back to Figure [2-1] and knowing that the change in temperature with respect to position (dT/dx) in front of and behind the detonation wave is equal to zero, specific conservation equations can be derived. These equations relate the thermodynamic and fluid dynamic properties between the two regions of the reference frame. These equations are:

$$\rho_1 u_1 = \rho_2 u_2 = const. = \dot{m} \qquad [2\text{-}11]$$

$$p_1 + \rho_1 u_1^2 = p_2 + \rho_2 u_2^2 \qquad [2\text{-}12]$$

$$C_p T_1 + \frac{u_1^2}{2} + q = C_p T_2 + \frac{u_2^2}{2} \qquad [2\text{-}13]$$

Using equation [2-4] and [2-5], equation [2-12] can be written as

$$h_1 + \frac{u_1^2}{2} = h_2 + \frac{u_2^2}{2} \qquad [2\text{-}14]$$

The fourth and final equation needed for deriving the Hugoniot relation is found in the assumption that the gases in both the burned and unburned regions behave like a perfect

$$p = \rho RT \qquad [2\text{-}15]$$

gas. The perfect gas law is defined for both regions and R is the specific gas constant for the reactants. Equations [2-11], [2-12], [2-14] and [2-15] are the basis set of equations

used to solve the five unknowns of the system, u_1, u_2, ρ_2, T_2, and p_2. One equation with two unknowns (ρ_2, p_2) can be formed by manipulating the four basis equations in the following manner:

$$p_2 - p_1 = \rho_1 u_1^2 - \rho_2 u_2^2 = \frac{(\rho_1 u_1)^2}{\rho_1} - \frac{(\rho_2 u_2)^2}{\rho_2} \qquad [2\text{-}16]$$

Substituting equation [2-7] in to [2-16] yields

$$\frac{(\rho_1 u_1)^2}{\rho_1} - \frac{(\rho_2 u_2)^2}{\rho_2} = \left(\frac{1}{\rho_1} - \frac{1}{\rho_2}\right)\dot{m}^2 \qquad [2\text{-}17]$$

Therefore,

$$\rho_1 u_1^2 = \frac{p_2 - p_1}{\frac{1}{\rho_1} - \frac{1}{\rho_2}} = \dot{m}^2 \qquad [2\text{-}18]$$

Equation [2-18] is the Rayleigh-line relation, which quantitatively describes the heat addition process in relation to velocity (u), pressure (p), and density (ρ) in a gas. Rearranging the Rayleigh-line relation in terms of Mach number (M) is a more useful way to describe the characteristics of the thermodynamics. This is done with the following approach:

$$M = \frac{u}{c} \qquad [2\text{-}19]$$

Where,

$$c = \sqrt{\gamma RT} \qquad [2\text{-}20]$$

Substituting equation [2-15] gives,

$$c = \sqrt{\frac{\gamma p}{\rho}} \qquad [2\text{-}21]$$

Manipulating equation [2-18] and substituting in equation [2-21], the Rayleigh-line relation becomes:

$$\frac{\gamma}{\gamma}\frac{\rho_1^2 u_1^2}{\rho_1 p_1} = \frac{\frac{p_2}{p_1} - 1}{1 - \frac{\rho_1}{\rho_2}} = \gamma M_1^2 \qquad [2\text{-}22]$$

Knowing that,

$$C_p - C_v = R \Rightarrow C_p = \frac{R}{1 - \frac{1}{\gamma}} = \left(\frac{\gamma}{\gamma - 1}\right)R \qquad [2\text{-}23]$$

equation [2-13] can be rewritten as,

$$\frac{\gamma}{\gamma - 1}\left(\frac{p_2}{\rho_2} - \frac{p_1}{\rho_1}\right) - \frac{1}{2}\left(u_1^2 - u_2^2\right) = q \qquad [2\text{-}24]$$

Using equation [2-12] to create an expressions for u_1^2 and u_2^2, and substituting into equation [2-24], the relation becomes,

$$\frac{\gamma}{\gamma - 1}\left(\frac{p_2}{\rho_2} - \frac{p_1}{\rho_1}\right) - \frac{1}{2}\left(\frac{p_2 - p_1}{\rho_1} + \frac{\rho_2}{\rho_1}u_2^2 + \frac{p_2 - p_1}{\rho_2} - \frac{\rho_1}{\rho_2}u_1^2\right) = q \qquad [2\text{-}25]$$

Combining equations [2-11] and [2-25] gives the final relation, equation [2-26], between heat addition and the gases initial and final pressures and densities.

$$\frac{\gamma}{\gamma - 1}\left(\frac{p_2}{\rho_2} - \frac{p_1}{\rho_1}\right) - \frac{1}{2}\left(p_2 - p_1\right)\left(\frac{1}{\rho_1} + \frac{1}{\rho_2}\right) = q \qquad [2\text{-}26]$$

This relation can also be written, with some manipulation of equation [2-4], [2-5] and [2-15] and substituting into equation [2-26].

$$h_2 - h_1 = \frac{1}{2}\left(p_2 - p_1\right)\left(\frac{1}{\rho_1} + \frac{1}{\rho_2}\right) \qquad [2\text{-}27]$$

These final two equations are forms of the Rankine-relation, but formally named for Hugoniot who derived them and fit the various combustion conditions to the pressure versus specific volume ($1/\rho$) curve.

The Hugoniot curve is a plot that describes the different possible combustion conditions. These combustion conditions include various strengths of deflagrations and detonations dependent upon the pressure and specific volume conditions at which the event is occurring. The Chapman-Jouget points described earlier can be plotted on this graph and prove to be the boundaries for strong and weak combustion events. Figure [2-2] is the Hugoniot curve along with a depiction of the different sections and boundaries of combustion events. The origin of the Hugoniot curve is labeled *A* and is constructed by

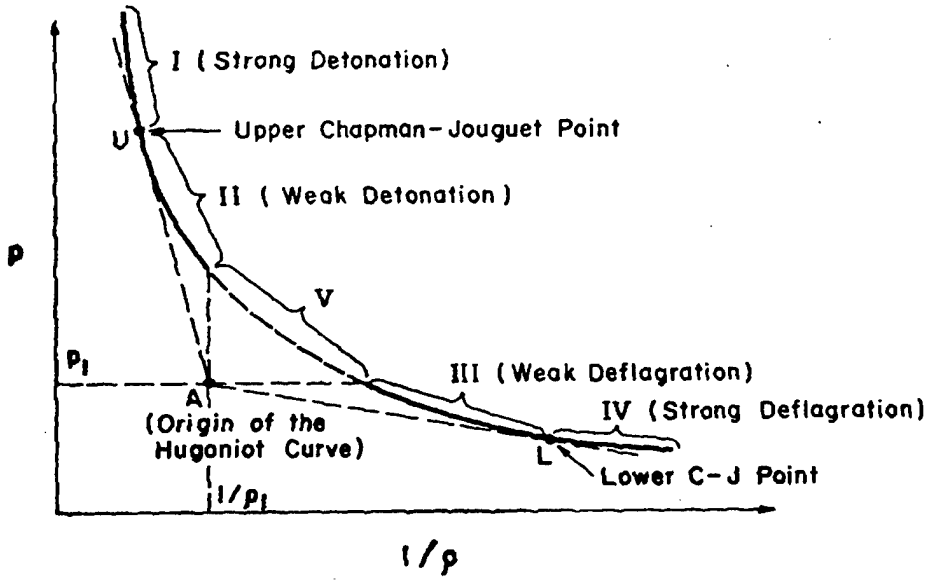

Figure [2-2]. Hugoniot Curve Depicting Different Combustion Regions. [From Ref. 2]

intersecting the tangents to the upper (*U*) and lower (*L*) C-J points. The combustion regions for both detonations and deflagrations can be described as both strong and weak, as depicted by regions I through IV in Figure [2-2]. Region V is a portion of the curve

that is physically impossible in that it needs u_1 to be imaginary to satisfy the Rayleigh-line relation. However, the region of interest for studying detonation transitions lies near the upper C-J point. It can be shown, and will be seen in the discussion of the detonation wave structure, that a detonation tends to naturally occur at this critical point on the Hugoniot curve. [Ref. 2]

2. Structure of a Detonation Wave

A detonation wave is sustained through a complex balance between a shock wave and the combustion event behind it. This symbiotic relationship is best understood through a one-dimensional analysis of a detonation wave. Three scientists completed the analysis independently in the early 1940's. Zel'dovich, von Neumann, and Doring believed the detonation wave could be viewed as three distinct regions whose widths are heavily dependent on the equivalence ratios and kinetics of the gaseous mixture. Figure [2-3] is a depiction of the thermodynamic properties in the three regions of the commonly named ZND detonation wave structure. The first region, the shock wave, has a width of just a few Angstroms, yet delivers a tremendous amount of energy into the unburned reactants seen as increases in pressure, density, and temperature. The dramatic increase in the thermodynamic properties increases the chemical reaction rates and accelerates the energy release phase of the wave structure. The deflagration region is made of two zones that describe the thermodynamics of combusting the reactants. The first, which is known as the Induction zone, has a relatively short width in which the chemical reaction is beginning but not yet impacting the thermodynamic properties. This shifts to the Reaction zone when the reaction rate increases exponentially, driving temperatures up and stabilizing pressure and density to their final equilibrium values. These three zones

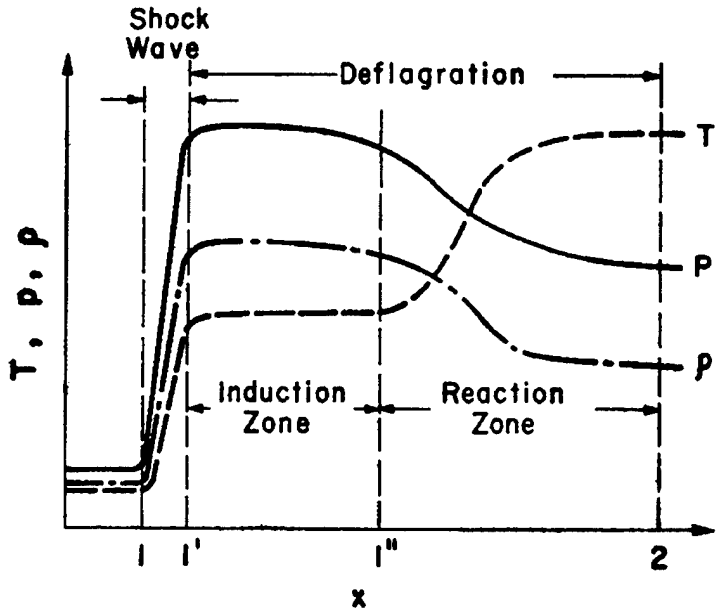

Figure [2-3]. Physical Properties of the 1-D Detonation Wave Structure. [From Ref. 2]

all occur within a distance on the order of a centimeter and each is dependent on the next to sustain the detonation wave.

D. THERMODYNAMIC EFFICIENCIES

1. Increased Thermal Efficiency of a Detonation Wave

The motivation for utilizing detonations as a means of propulsion is the possibility of increased efficiency. This is not surprising because nearly all significant breakthroughs in combustion engines have come in the form of decreasing the thermodynamic losses within the engine. Thermodynamically, the efficiency of any system is directly related to its ability to minimize the entropy rise in the working fluid. Therefore, a careful analysis of the entropy budget must be completed to justify further research in detonations as a means of propulsion.

An expression for the entropy (s) of a combustion event can be derived from the Hugoniot relationship discussed earlier. In order to prove the increased efficiency of a detonation, the entropy at the upper C-J point on the Hugoniot curve must be analyzed.

Kuo, in *Principles of Combustion*, describes this derivation in the following steps [Ref. 2]. To begin, the energy of the system must be defined and well understood. The enthalpy (h) is defined as

$$h \equiv e + \frac{p}{\rho} \qquad [2\text{-}28]$$

where e is the total internal energy within the system. Applying this two the 1-D stationary detonation wave, equation [2-28] becomes

$$h_2 - h_1 = (e_2 - e_1) + \left(\frac{p_2}{\rho_2} - \frac{p_1}{\rho_1}\right) \qquad [2\text{-}29]$$

Substituting equation [2-29] into the Hugoniot relation, equation [2-27], and sorting terms gives

$$(e_2 - e_1) = \frac{1}{2}(p_2 - p_1) + \left(\frac{1}{\rho_2} - \frac{1}{\rho_1}\right) \qquad [2\text{-}30]$$

Differentiating,

$$de_2 = \frac{1}{2}(dp_2)\left(\frac{1}{\rho_1} - \frac{1}{\rho_2}\right) - \frac{1}{2}\left(d\frac{1}{\rho}\right)(p_2 + p_1) \qquad [2\text{-}31]$$

Combining the first and second laws, the following expression can be generated which introduces entropy into the analysis.

$$T_2 ds_2 = de_2 + p_2 d\left(\frac{1}{\rho_2}\right) \qquad [2\text{-}32]$$

Substituting equation [2-31] into [2-32] and rearranging terms, gives an expression in terms of a change in entropy over a change in specific volume

$$T_2 \frac{ds_2}{d(1/\rho_2)} = \frac{1}{2}\left(\frac{1}{\rho_1} - \frac{1}{\rho_2}\right)\left(\frac{dp_2}{d(1/\rho_2)} - \frac{p_2 - p_1}{\frac{1}{\rho_2} - \frac{1}{\rho_1}}\right) \qquad [2\text{-}33]$$

Analyzing the Hugoniot curve at the upper and lower Chapman-Jouget points, the slope of the tangents to the curve at these points is

$$\left(\frac{dp_2}{d(1/\rho_2)}\right)_{C-J} = \frac{p_2 - p_1}{\frac{1}{\rho_2} - \frac{1}{\rho_1}} \qquad [2\text{-}34]$$

Therefore, when equation [2-34] is applied to equation [2-33] representing the conditions at the upper and lower C-J points, it becomes

$$\left(\frac{ds_2}{d(1/\rho_2)}\right)_{C-J} = 0 \qquad [2\text{-}35]$$

This result indicates that the entropy value on the Hugoniot curve at the C-J points is either a maximum or a minimum. In order to determine what the condition is, the second derivative in entropy must be taken.

$$T_2\left(\frac{d^2 s_2}{d(1/\rho_2)^2}\right)_{C-J} = \frac{1}{2}\left(\frac{1}{\rho_1} - \frac{1}{\rho_2}\right)\left(\frac{d^2 p_2}{d(1/\rho_2)^2} - \frac{1}{\left(\frac{1}{\rho_2} - \frac{1}{\rho_1}\right)}\frac{dp_2}{d(1/\rho_2)} + \frac{p_2 - p_1}{\left(\frac{1}{\rho_2} - \frac{1}{\rho_1}\right)^2}\right)_{C-J} \qquad [2\text{-}36]$$

Isolating the second derivative in entropy and using the condition outlined in equation [2-34], equation [2-36] reduces to

$$\left(\frac{d^2 s_2}{d(1/\rho_2)^2}\right)_{C-J} = \frac{1}{2T_2}\left(\frac{1}{\rho_1} - \frac{1}{\rho_2}\right)\left(\frac{d^2 p_2}{d(1/\rho_2)^2}\right)_{C-J} \qquad [2\text{-}37]$$

A separate analysis of the asymptotes of the Hugoniot curve shows the second derivative of pressure in equation [2-37] is greater than zero.

$$\frac{d^2 p_2}{d(1/\rho_2)^2} > 0 \qquad [2\text{-}38]$$

Using this fact and knowing the difference between the specific volumes at the upper and lower C-J points, it can be determined which point maximizes entropy and which minimizes it. For deflagrations the specific volume ($1/\rho_1$) behind the shock front is less than that behind it ($1/\rho_2$). Therefore for $1/\rho_1 < 1/\rho_2$

$$\left(\frac{d^2 s_2}{d(1/\rho_2)^2}\right)_{LowerC-J} < 0 \qquad [2\text{-}39]$$

which corresponds to a post combustion condition with the highest entropy rise for a specified amount of heat addition, at the lower C-J point. Conversely, at the upper C-J point, analogous to the detonation, the opposite holds true. At this point $1/\rho_1 > 1/\rho_2$, resulting in

$$\left(\frac{d^2 s_2}{d(1/\rho_2)^2}\right)_{UpperC-J} > 0 \qquad [2\text{-}40]$$

which corresponds to a post combustion condition with the lowest entropy rise for a specified amount of heat addition. Figure [2-4] is a graphical representation of the entropy variation over the entire Hugoniot curve. This analysis demonstrates the increased amount of work available and efficiency of the detonation process over deflagration combustion events

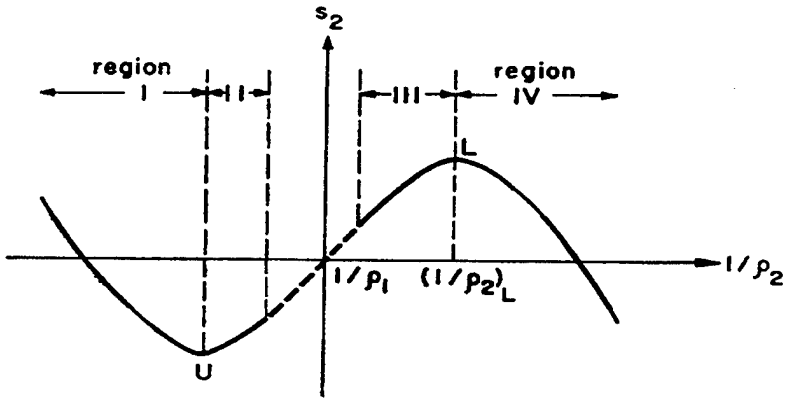

Figure [2-4]. Entropy Variation Along the Hugoniot Curve. [From Ref. 2]

2. Engine Cycle Analysis Comparison

a. *Comparison Approach*

A practical approach to demonstrating the increased thermodynamic efficiency of a Pulse Detonation Engine (PDE) is to compare the two idealized combustion processes that could be utilized for heat addition. This section will perform a cycle analysis on a constant pressure (C_p) combustion, currently used by turbojets, ramjets, etc., and a detonation (C-J) cycle, which exists for a PDE system. Both cycles will be analyzed as ideal with the understanding they will not completely model the performance limit of a real world engine. The approach will, however, bound the real world benefits of a PDE cycle. This section will review the goals, assumptions, and equations needed to outline the analysis for each cycle.

The ultimate goal of this analysis is to compare two idealized combustion cycles using the First Law of Thermodynamics and reveal the increased thermodynamic efficiency of a detonation combustion cycle. In doing this, a baseline understanding of the fundamental differences between C_p and C-J cycles will be presented. This analysis will also build a solid thermodynamic approach to each cycle. The result will be a simple thermodynamic analysis for the Pulse-Detonation Engine (PDE) cycle.

The analysis involves several assumptions of the combustion parameters and cycle behavior. The working fluid that will be used is an Ethylene (C_2H_4) and air gas mixture at stoichiometric conditions. The stoichiometric condition is defined as the mixture's fuel to air ratio that facilitates complete combustion, leaving no fuel or oxidizer in the combustion products. A mixture's equivalence ratio is based on the reactant's actual fuel to air ratio divided by that of the stoichiometric condition. The mixture is assumed to behave in accordance with the perfect gas law,

$$pv = RT \qquad [2\text{-}41]$$

The mixture will be treated as thermally and calorically perfect with constant specific heats through the isentropic portions of the cycle. This allows the enthalpy (h) and internal energy (u) to be functions of temperature (T) only,

$$h = C_p \int dT \qquad [2\text{-}42]$$

The energy released by the combustion process will be assumed to be simple heat addition ($q_{1\text{-}2}$) based on the type of combustion process for the cycle. Further assumptions must be placed on the cycles in order to standardize them for a coherent analysis. Both cycles are started with an initial condition equivalent to that of an operating system at an altitude of 50,000 ft., and will be labeled as state (0). Next, both the compression (0-1) and expansion (2-4) paths will be modeled as isentropic. The heat addition path occurs between state (1) and (2) and will be supplied by the combustion process. The cycle will be completed by a constant pressure cooling which is physically seen as a new load of reactants at the initial condition along the (4-0) path. Figure [2-5] is a generalized plot of a combustion cycle to outline the four paths within the cycle.

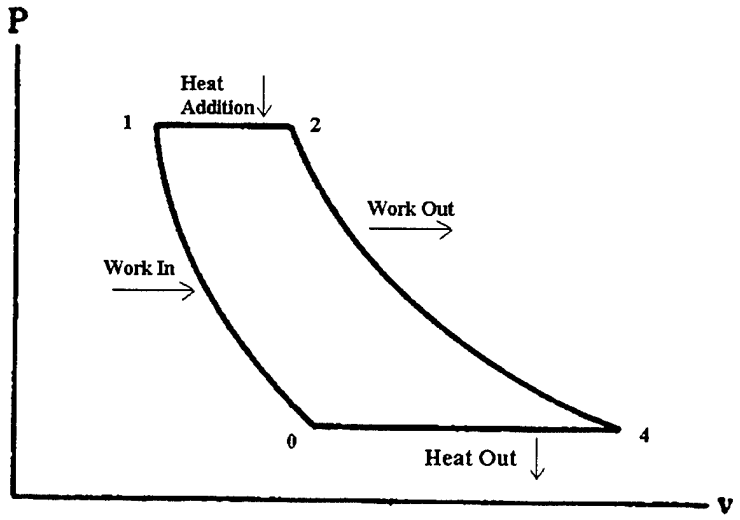

Figure [2-5]. P-v Diagram of Generalized Combustion Cycle.

It will be shown by careful analysis that this plot shifts with different combustion events that correspond to differences in the total work output and efficiency of the cycle. Table [2-2] outlines the state (1) parameters that will be used for each cycle [Ref. 7]. Each cycle will assume an initial compression ratio of 10:1. Parameters at each state of the cycles will be given during the analysis. These values will make it possible to calculate the work and efficiency of that cycle in order to adequately compare them.

Table [2-2]. Standard Parameters for Combustion Cycle Analysis. [From Ref. 7]

Parameter	Symbol	Value	Units
Ratio Specific Heat	γ	1.35	None
Specific Heat (constant pressure)	C_p	1.04	kJ/kg
Standard Temperature	T	300.00	K
Standard Pressure	p	1.0	atm
Specific Volume	v	0.8	m^3/kg
Entropy	s	6.48	kJ/kgK

The equations utilized for the analysis are derived from the basic laws of physics and thermodynamics. As previously outlined, the conservation of mass,

momentum and energy along with the second law of thermodynamics are required to perform the cycle analysis. These equations in cycle notation are presented again for convenience:

Conservation of mass: $$\rho_1 u_1 = \rho_2 u_2 = \dot{m} \quad [2\text{-}43]$$

Conservation of momentum: $$\rho_1 u_1^2 + p_1 = \rho_2 u_2^2 + p_2 \quad [2\text{-}44]$$

Conservation of energy: $$h_1 + \frac{u_1^2}{2} + q_{1\to 2} = h_2 + \frac{u_2^2}{2} \quad [2\text{-}45]$$

Or $$u_1' + p_1 v_1 + \frac{u_1^2}{2} + q_{1\to 2} = u_2' + p_2 v_2 + \frac{u_2^2}{2} \quad [2\text{-}46]$$

substituting in the relation,

$$h = u' + pv \quad [2\text{-}47]$$

The second law of thermodynamics combined with the Gibb's free energy function will also be utilized to determine the entropy between the phases of the cycles. It follows the form,

$$s = C_p \ln\left(T/T_{Ref}\right) - R\ln\left(p/p_{Ref}\right) \quad [2\text{-}48]$$

Another relation that defines how a combustible gas will behave in a given cycle is that it must follow the Hugoniot curve and Rayleigh line relation defined earlier in Section C of this chapter. The curves define all the mathematically possible end states for a gas with the specified amount of heat release and initial conditions, although only certain regions of the curve are attainable. The curves are hyperbolic in form and, by manipulating the three conservation equations, the velocity of the gas dependence can be removed. All of these relations must be satisfied for a given combustion process to occur in nature, and using them will produce the cycle parameters required for evaluating cycle efficiency.

Combustion cycle efficiency will be calculated thermodynamically using the standard definition,

$$\eta_{TH} = \frac{W_{net}}{q_{addition}} \qquad [2\text{-}49]$$

However, the total work of the cycle must be calculated first. This will be done utilizing the conservation of energy principle.

$$\oint \delta W = \oint \delta q \qquad [2\text{-}50]$$

By solving for the total work produced by the combustion cycle, the thermal efficiency can be solved by knowing the amount of heat released from the reactants during the combustion event. The thermal efficiency of both cycles will be conducted to determine the possible thermodynamic gains a detonation based cycle could give in a propulsion system.

b. *Deflagration at Constant Pressure Analysis*

This analysis will step through the procedure used to determine the state values through a constant pressure combustion cycle. The initial conditions used for all calculations is outlined in Table [2-2] at the pre-combustion state (1). To solve for the initial state (0), the isentropic relationship, shown by equation [2-51], coupled with the 10:1 compression ratio is used. The temperature at state (0) is then solved for utilizing the perfect gas law shown by equation [2-41].

$$P v^{\gamma} = Const. \qquad [2\text{-}51]$$

To solve for the post-combustion state (2), the thermodynamic code *TEP* was run for constant pressure conditions with the defined reactant ratios [Ref. 8]. The output from *TEP* provided the post-combustion temperature, γ, C_P, and entropy of the mixture.

Assuming the products behave as a perfect gas, the specific volume for the state can be solved using the perfect gas law. The properties at state (4), are arrived at through an isentropic expansion and are solved for using the same isentropic analysis used for the compression process. Table [2-3] depicts the results of this analysis. A pressure-specific volume (P-v) diagram, shown in Figure [2-6], displays the constant pressure combustion cycle. This diagram can be used to compare the constant pressure cycle with the C-J detonation cycle.

Table [2-3]. State Parameters for a Constant Pressure Combustion Cycle.

State	Pressure (atm)	Temperature (K)	v (m^3/Kg)	entropy (*s*) (KJ/Kg-K)
0	0.1	164.9	5.3	6.5
1	1.0	300.0	0.8	6.5
2	1.0	2353.0	6.2	9.6
4	0.1	1361.1	39.3	9.6

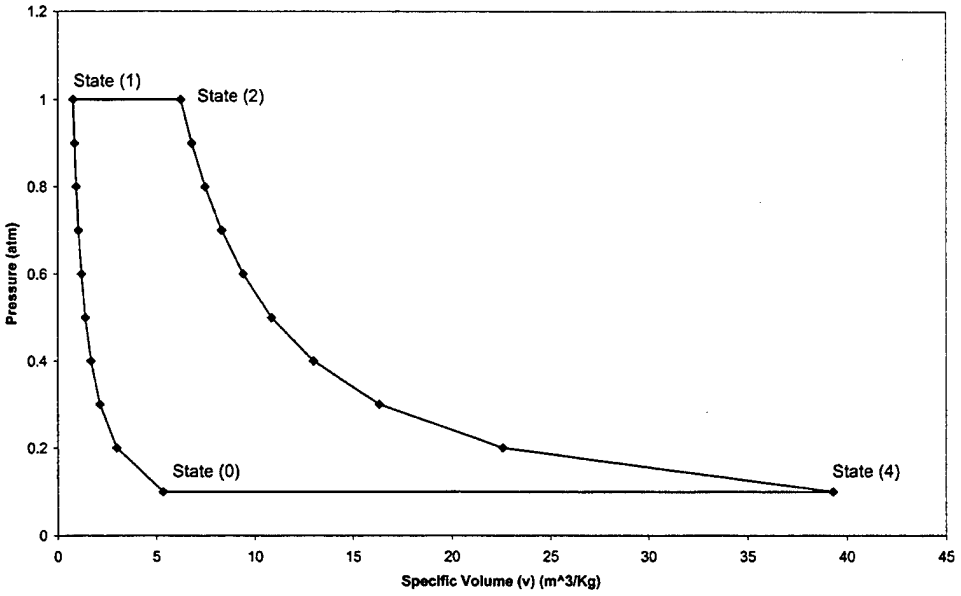

Figure [2-6]. P-v Diagram of Constant Pressure Combustion Cycle.

The constant pressure combustion cycle's thermal efficiency calculation requires the heat added by the combustion to be determined. The difference between the pre-combustion and post-combustion enthalpies were calculated to determine this value.

The conservation of energy equation shows that this difference is equal to the heat added to the reactants from combustion. Equation [2-52] depicts this calculation and is derived by manipulating equations [2-42] and [2-45] and assuming no change in the reactants velocity.

$$C_{P2}T_2 - C_{P1}T_1 = h_f^\circ = q_{1\to 2} \qquad [2\text{-}52]$$

From this calculation, the heat added by combustion (q_{12}) is equal to 3105.1 (KJ/Kg-K). The heat released to the atmosphere is calculated, assuming a constant post-combustion C_p, using equation [2-53].

$$C_{P2}T_2 - C_{P1}T_1 = q_{4\to 0} \qquad [2\text{-}53]$$

The net work (W_{net}) of the cycle is then calculated to be 1749.2 (KJ/Kg-K). Using equation [2-49], the thermal efficiency (η_{TH}) of the idealized constant pressure combustion cycle is calculated to be 41.9%.

c. *Detonation Analysis*

This analysis will step through the procedure used to determine the state values through a C-J combustion cycle. In order to adequately compare the C-J cycle to the constant pressure cycle, the same initial pre-combustion compression ratios were used. The properties for states (1) and (2) were found utilizing the same procedure outlined in Section D.2.c. To solve for the post-combustion state (3), the thermodynamic code *TEP* was run under detonation conditions with the defined reactant ratios [Ref. 8]. Again, assuming the products behave as a perfect gas, the specific volume for the state was solved for using the perfect gas law. The properties at state (4), were determined through an isentropic expansion and are solved for using the same isentropic analysis used for the compression process. Table [2-4] depicts the results of this analysis. A

pressure-specific volume (P-v) diagram, shown in Figure [2-7], displays the C-J detonation cycle and can be used to compare the cycle with the C_P combustion cycle.

Table [2-4]. State Parameters for a C-J Detonation Cycle.

State	Pressure (atm)	Temperature (K)	v (m^3/Kg)	entropy (*s*) (KJ/Kg-K)
0	0.1	164.9	5.3	6.5
1	1.0	300.0	0.8	6.5
2	18.2	2926.0	0.4	9.2
4	0.1	1022.9	27.2	9.2

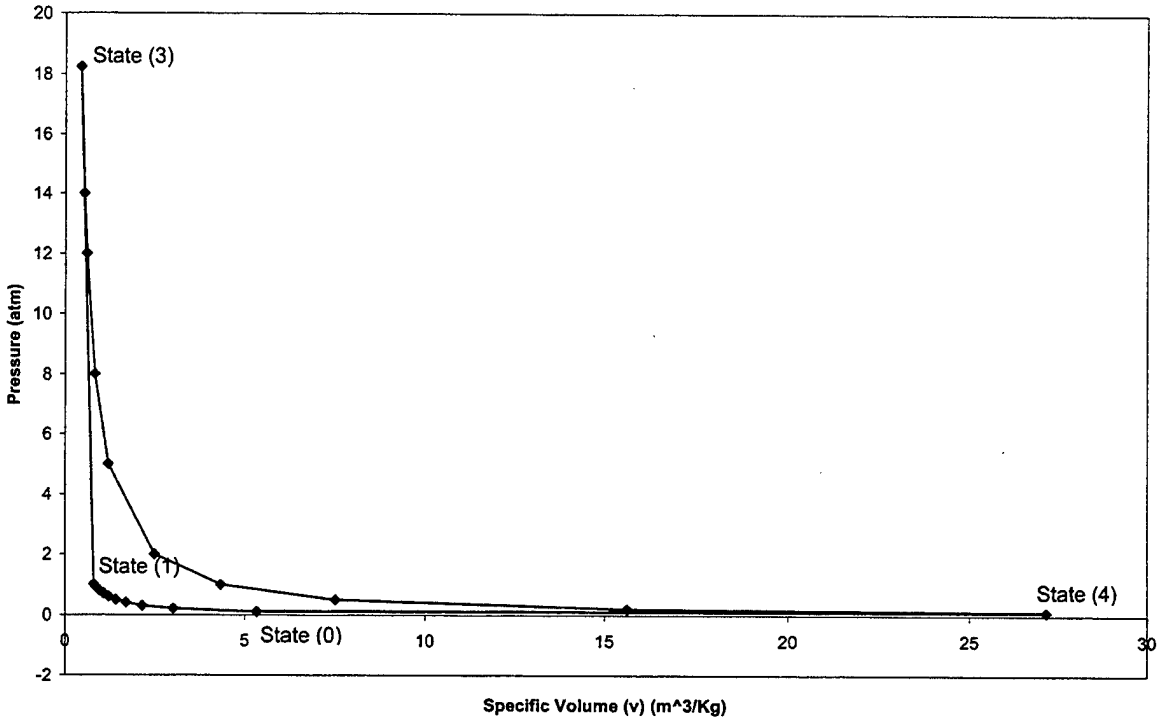

Figure [2-7]. P-v Diagram of C-J Detonation Cycle.

The detonation cycle's thermal efficiency was determined by analyzing the differences in the enthalpies in the pre and post-combustion states. The thermodynamic conservation of energy shows that this difference is also equal to the heat added to the working fluid from the combustion process. Equation [2-54] is derived by manipulating equations [2-42] and [2-45]. However, in a detonation the velocities of the reactants

contain a substantial amount of energy and cannot be ignored for the calculation. For an assumed stationary combustion wave, the equation becomes:

$$C_{P2}T_2 + \frac{(V_{det} - c)^2}{2} - C_{P1}T_1 - \frac{V_{det}^2}{2} = h_f^\circ = q_{1\to 2} \qquad [2\text{-}54]$$

This calculation determines the heat added by combustion (q_{12}) to be equal to 2960.7 (KJ/Kg-K). The heat released to the atmosphere was calculated assuming a constant post-combustion C_p and using equation [2-55].

$$C_{P2}T_4 - C_{P1}T_0 = q_{4\to 0} \qquad [2\text{-}55]$$

With these values known, the net work (W_{net}) of the cycle was then calculated to be 1758.2 (KJ/Kg-K). By equation [2-49], the thermal efficiency (η_{TH}) of the idealized constant pressure combustion cycle equals 65.6%.

3. Thermodynamic Analysis Results

The analysis carried out in the previous two sections analyzed two separate combustion processes at the same initial conditions. The results of the analysis depict a substantial difference in the overall thermal efficiency of the two cycles. Table [2-5] is a summary of the important efficiency parameters, η_{TH}, entropy change (Δs), and the percent difference between the two cycles.

Table [2-5]. Efficiency Comparison of Detonation and C_P Combustion Cycles.

	η_{TH}	Δs (KJ/Kg-K)
Constant Pressure Combustion	41.9	3.1
C-J Detonation	65.6	2.7
Percent Difference	56.6 %	-12.9 %

A graphical display of the difference in the net work can be seen in the integration under the P-v diagrams for both cycles. The C-J combustion process gains its advantage in the nearly constant volume combustion that drives the pressure 18 times that of the

constant pressure combustion. Figure [2-8] displays these differences, which can be seen by comparing the areas under each curve, which represents the net work. Another, more classical, way to compare the two cycles is to look at the net efficiency gain for each. Following the theory outlined in Section D.1 of this chapter, the C-J detonation cycle results in a significantly lower entropy rise, which results in more work available. For this reason the Pulse Detonation Engine concept is a theoretically attractive alternative for a high-speed long-range propulsion system.

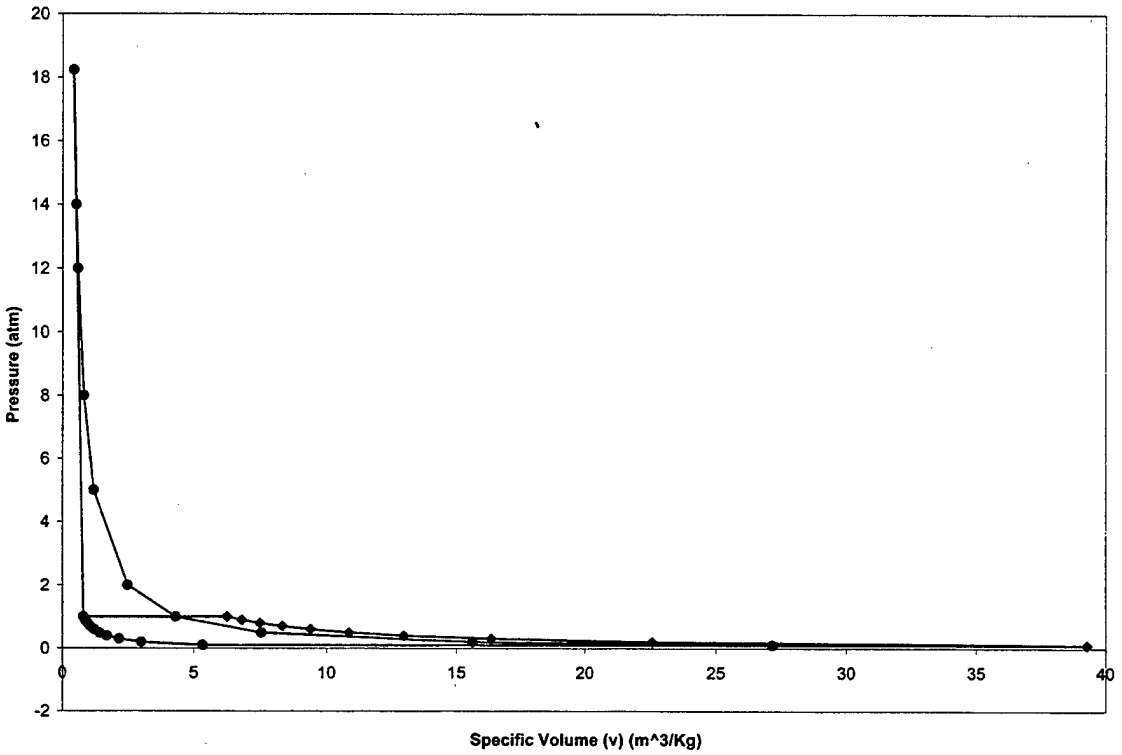

Figure [2-8]. P-v Diagram Comparison of C-J Detonation vs. Cp Combustion Cycle.

E. PHYSICAL MECHANICS OF A DETONATION

1. Deflagration-to-Detonation Transition

The goal of this research is to determine conditions for minimum deflagration-to-detonation transition (X_{DDT}) distance in a simple tube combustor with one open end. In

order to quantitatively measure this parameter, the concept of transitioning to a detonation wave must be understood. Kuo describes the sequence of events leading to a fully developed detonation wave in four generalized steps.

- First, laminar flames of an enclosed deflagration produce compression waves that coalesce to form a shock front in the unburned reactants.
- This shock front creates a turbulent reaction zone within the flame front, which eventually causes an "explosion within an explosion" behind the shock front.
- This "explosion" produces strong shock waves in both directions and oscillations between them, called transverse waves. The rearward propagating shock is called a retonation while the forward shock is known as a superdetonation.
- Interactions between all of these events coupled with the reaction zone of the primary flame front combine to create a steady state supersonic C-J detonation wave.

Figures [2-9] and [2-10] are depictions of this developing detonation wave process outlined above. [Ref. 2]

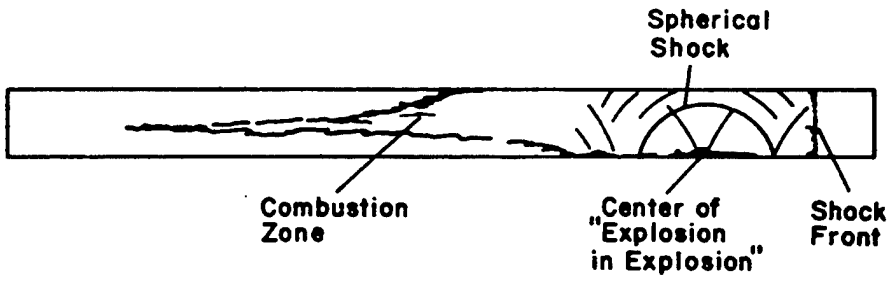

Figure [2-9]. "Explosion Within Explosion" in a Developing Detonation. [From Ref. 2]

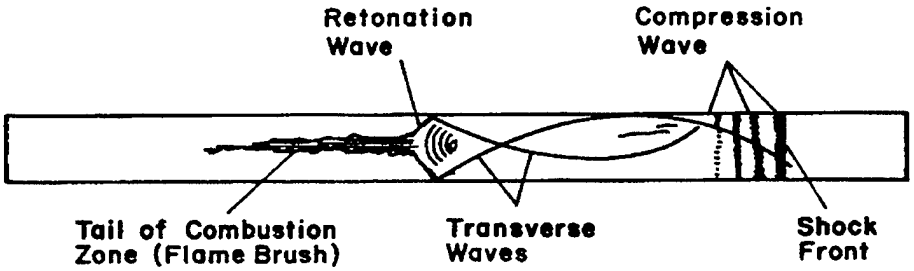

Figure [2-10]. Components of a Transitioning Detonation Wave. [From Ref. 2]

Experiments measuring the wall static pressure of the combustion wave front as it propagates down the combustor tube show that it is possible to determine where the wave transitions from a deflagration to a detonation. Figure [2-11] is a depiction of a typical transitioning detonation wave. Note the gradual rise in pressures and shock front speed in the first two transducers. This is indicative of the coalescing of shock waves in the transitioning process. Referring back to the ZND wave structure of a detonation, Figure [2-5], the fully developed detonation wave will show a sharp and drastic increase in pressure as it passes the transducer. This can be seen in the wave trace of transducer P5 shown in Figure [2-11]. That is the position at which the wave is determined to be fully transitioned. The retonation phenomena can be seen in the subsequent pressure peaks of P6 and P7 as the retonation propagates back over the transducers and reflects off the head wall of the combustor.

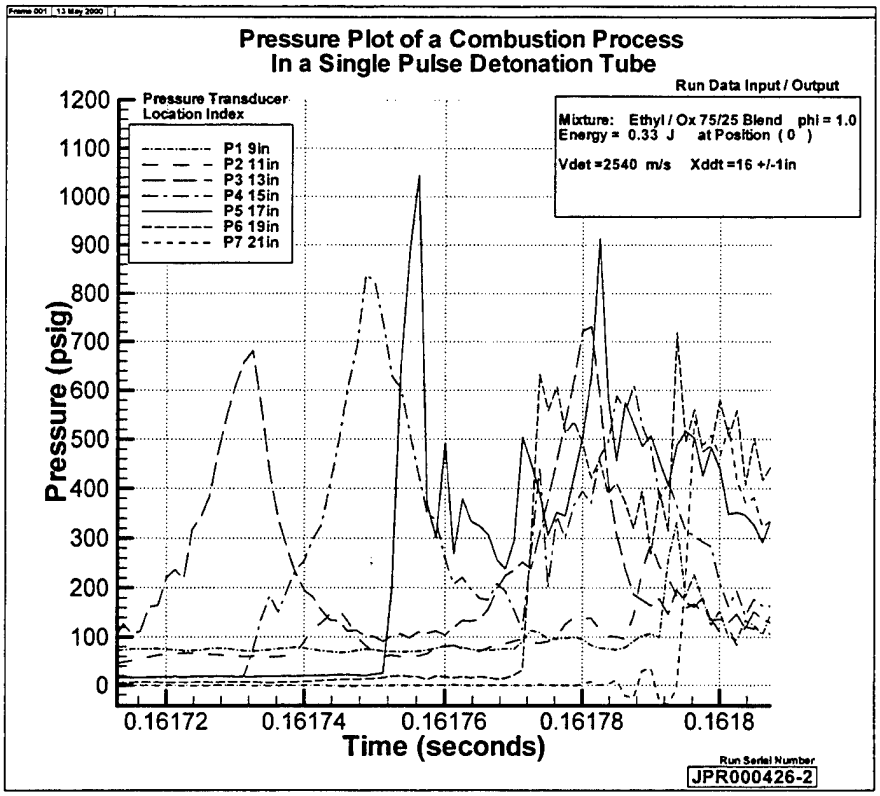

Figure [2-11]. Pressure Trace of a Transitioning Detonation Wave.

By analyzing the shapes and speeds of the wave at different points along the combustor, it is clear that the wave transitioned into a detonation between P4 and P5 transducers. Once transitioned, the wave continues to propagate at the steady-state C-J detonation velocity.

2. Detonation Wave Velocity

The key indication that a combustion event is a detonation is to measure its wave velocity and compare it with theoretical values. Detonation wave velocities can reach velocities of 1500-3000 meters per second dependent upon the chemical properties of the reactants. This detonation velocity, once reached, generally remains constant throughout the combustor. This fact is predicted by Chapman-Jouget theory of detonations and proven in well-documented experiments. This was also seen in the experiments conducted for this research. The detonation velocity (V_{det}) was determined using the

static pressure traces of the wave as it traveled through the combustor. The rate equation was used for this calculation by timing the wave as it passed over a known distance between transducers. Figure [2-12] depicts a detonation wave trace as it propagates over pressure transducers spaced 2 inches apart. This fact along with a measured time between them, allows the experimental V_{det} to be calculated to be 2822±180 meters per second for this particular run.

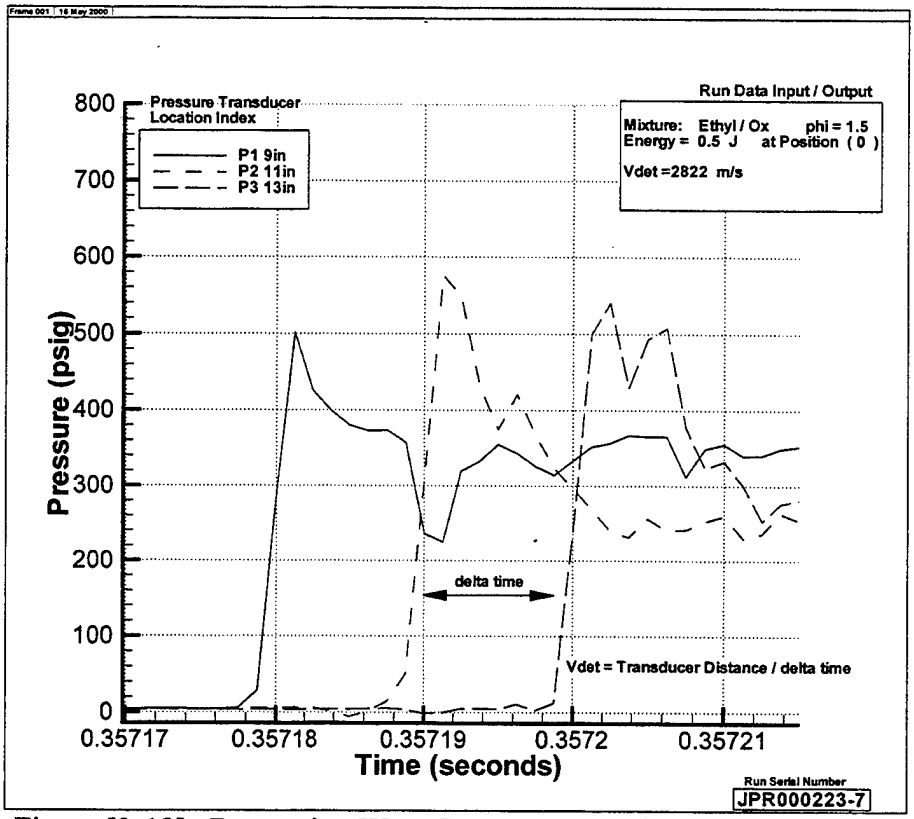

Figure [2-12]. Detonation Wave Pressure Trace for Calculating V_{det}.

Occasionally, speeds of 30% to 40% greater than theoretical velocities were seen in many of the experiments. This phenomenon is explained by the Von-Nuemann spike theory. He states that there is a short period of over pressurization and overdriven velocities generated at the onset of a detonation transition.

Once the wave speed is known using this technique, it can be compared to the theoretical values to determine if a detonation wave was present. The theoretical detonation wave velocity can be analytically determined using the formulas derived in Chapter II.C, however the computer code *TEP* quickly solves this problem for a given reactant mixture, equivalence ratio and combustor pressure and temperature parameters [Ref. 8]. Figure [2-13] is a plot of this comparison completed for ethylene/oxygen mixture at several equivalence ratios.

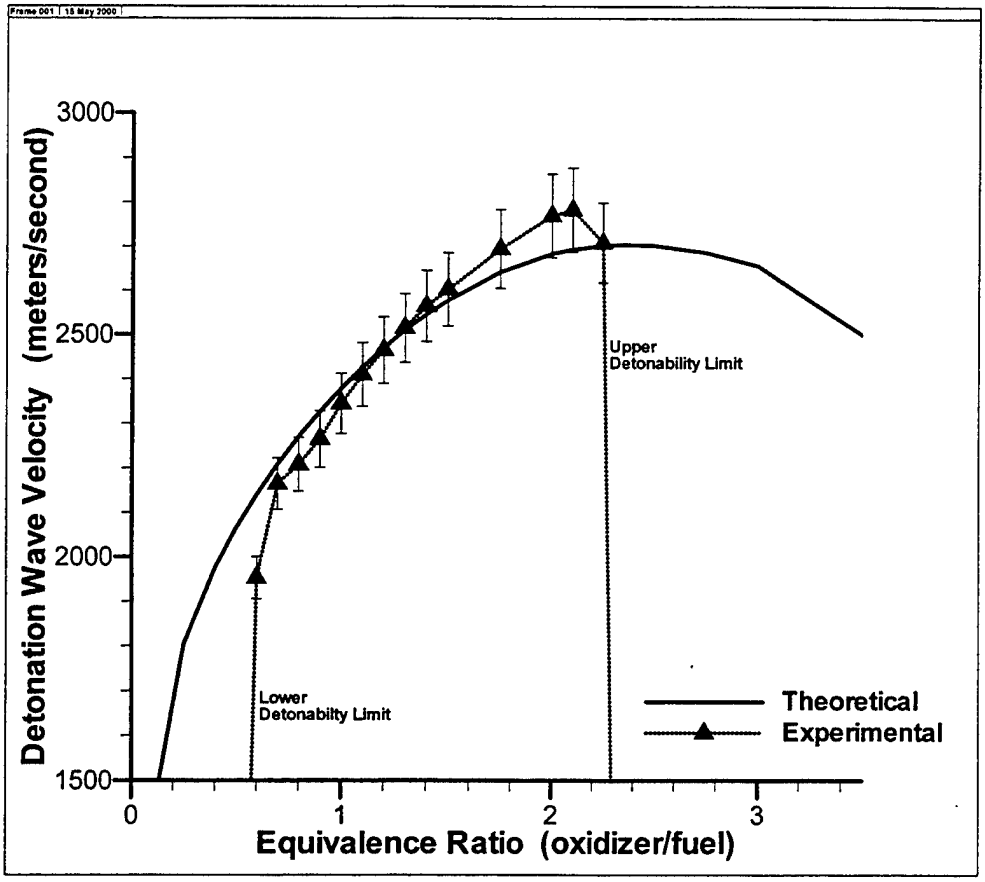

Figure [2-13]. Theoretical vs. Experimental Detonation Velocity Comparison.

The drastic fall off in wave velocities for the experimental cases at equivalence ratios of 0.6 and 2.2, show the observed detonability limits of the reactants for the geometry tested. The *TEP* code does not account for this limitation and carries out its calculations

with no physical meaning. The error bars in the plot quantify experimental error in the time and distance measurement of the propagating wave and vary with the wave's velocity. This error analysis is rigorously derived in Chapter IV.B.5. Once the combustion event is determined to be a detonation, the point at which the wave transitioned can be determined.

3. Ignition Source Level and Location

The ignition source parameters are the means by which the combustion event is initiated and play integral roles in the development of detonations. The initial energy provided is directly related to how quick the flame front becomes turbulent resulting in the deflagration-to-detonation transition. This energy may be provided by any number of means including a spark ignitor, focused acoustic energy, or by another detonation wave. The spark ignitor propagates a flame kernel hemi-spherically into the reactants initiating the flame front. A detonation that sparks another detonation in a separate mixture is called a pre-detonator, and is currently the means by which the larger combustors of PDEs are being initiated. Each type of ignition source drives a detonation transition at different distances. The key is to force the detonation to transition as early and simply as possible.

A means by which this is optimized is to focus the available energy into a smaller volume of reactants. This would theoretically create greater turbulence in the initial flame front, driving the detonation to transition earlier. This research will look into a simple focusing technique of superimposing the flame fronts of an ignitor spark. This will be accomplished by placing the ignitor along the combustor's sidewall at different locations. Once sparked, the flame front will propagate both forward and aft along the

combustor until the latter reflects back and coalesces with the forward wave. This creates a greater energy flux through the reactants forcing a detonation to occur earlier. If proven successful, other techniques of energy focusing may also prove to substantially decrease the deflagration-to-detonation transition distance.

4. Thrust Generated by a Detonation Wave

In order for a detonation combustion process to be used viably in a propulsion cycle, it must be able to provide a means of thrust. A look back to the C-J cycle analysis and experimental results give insight into this issue. A detonation in an open-ended tube type combustor produces significant pressure on the combustor's head wall. This pressure is derived from the post combustion properties of the products behind the detonation wave by performing a Taylor-Zeldovich expansion. The properties of the post detonation state in the cycle can be seen in Figure [2-7] as state (2) and the properties at the head wall as state (3). The pressure at the post detonation state (P_2) in the ethylene / oxygen mixture is calculated to be 18.7 atm or 274.9 psia. The expanded pressure at the head wall (P_3) is calculated using the Taylor-Zeldovich isentropic expansion relation shown by equation [2-56]. Using the post combustion specific heat ratio (γ_2), P_3 is calculated to be 135 psia.

$$P_3 = \left(\frac{\gamma+1}{2\gamma}\right)^{\frac{2\gamma}{\gamma-1}} P_2 \qquad [2\text{-}56]$$

The head wall pressure can also bee seen experimentally as shown by a pressure trace three inches from the head wall of a detonation as it propagates through the combustor. Figure [2-14] depicts this average head wall pressure generated by the detonation.

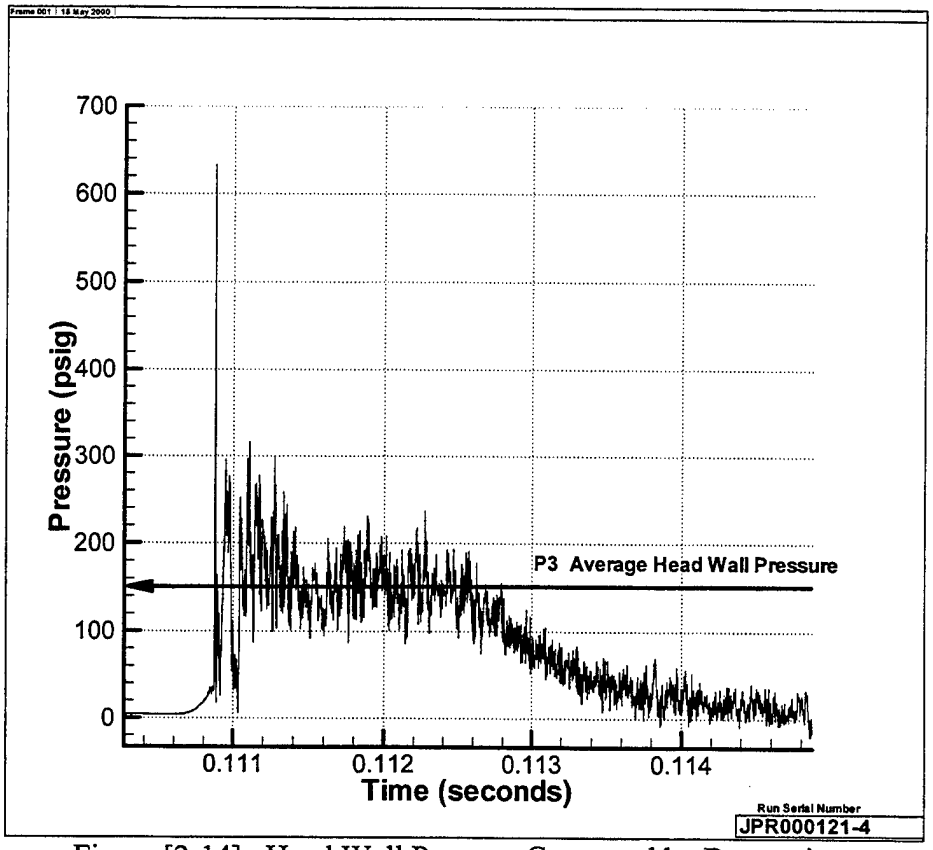

Figure [2-14]. Head Wall Pressure Generated by Detonation.

The average pressure of the combustion products (P_3) pressure in Figure [2-14], is 150 psig. This correlates to a momentary thrust level of 1060 lb for the three-inch diameter combustor. The gradual decay in pressure 1.35 milliseconds after the detonation wave passes corresponds to the corresponding isentropic blowdown process after the wave exits the combustor into the atmosphere. The short time period of the thrust is overcome by the use of a pulsed cycle. A pulse detonation engine will need to generate detonations at cycle rates of 100 Hz or more to produce the quasi steady-state thrust required by a flight vehicle.

THIS PAGE INTENTIONALLY LEFT BLANK

III. EXPERIMENTAL SETUP AND PROCEDURE

A. INTRODUCTION

The test facility is located at the Naval Postgraduate School's Rocket, Propulsion and Combustion Laboratory (RPCL) in Monterey, California. The test apparatus was designed and built specifically to investigate parameters that affect a transitioning detonation wave. The test cell in which the experiment was set up is a hardened bunker that is well protected against potentially serious accidents. The facility's hardware consists of a simple constant area tube combustor, a variable energy ignition system, control valves and pumps, and high-speed pressure transducers. The gases that made up the reactants were a detonable mixture of ethylene (C_2H_4), oxygen (O_2), and nitrogen (N_2). The control of all valves and data acquisition was provided by a Microsoft® Visual Basic GUI code developed specifically for this experiment [Ref. 9]. The four independent variables of the experiment, ignition energy, ignition location, stoichiometry, and oxygen (O_2) content, were evaluated in order to determine their effect on the deflagration-to-detonation transition distance

B. HARDWARE DESCRIPTION AND FUNCTIONS

1. Combustor Tube

The most important piece of hardware in the test facility was the combustor tube. The tube was 75 inches long and 3 inches in inside diameter and made of type-316 stainless steel. It consists of two individual sections connected by a flange assembly to allow for different test conditions. Thirty-three test ports are used to place pressure transducers along the inner surface of the tube wall. There are also ports placed along the

tube wall to allow for injection and extraction of the reactants during a test. The tube is secured and supported laterally by two notched braces and longitudinally by a thrust wall at its head end to absorb the impulse force generated by the detonation. Each brace is mounted to a massive stationary test table. Figure [3-1] is a photograph of the combustor tube with all its support equipment.

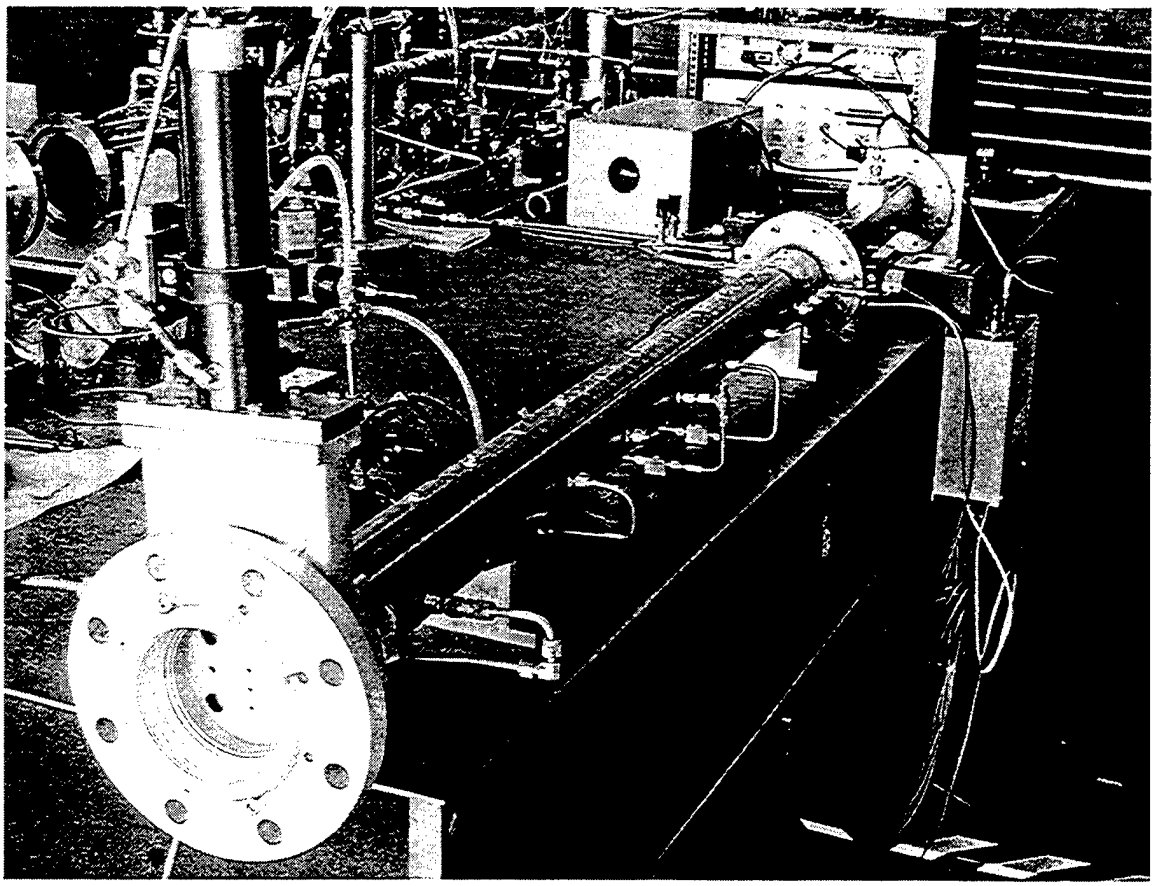

Figure [3-1]. Detonation Tube Combustor with Support Equipment.

2. Variable Ignition System

An important component evaluated in this experiment was the ability to accurately vary the ignition source energy delivered to the reactants within the combustor. This was effectively accomplished using the Unison manufactured Vision-8

Variable Ignition System (VIS-8). Figure [3-2] is a photograph of the Vision-8 system with the ignitor installed into the combustor.

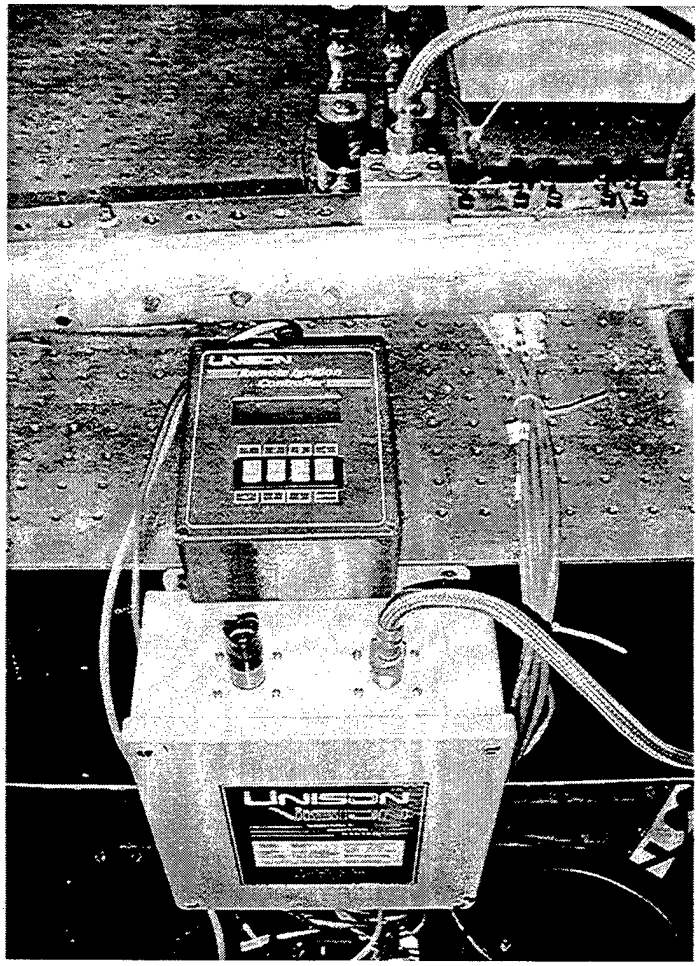

Figure [3-2]. Unison Vision-8 Variable Ignition System.

The ignition energy delivered to the ignitor could be varied from 0.33 to 8.31 Joules. The energy delivered to the reactants is substantially less due to the manner in which a capacitive discharge system works. These losses are nominally 75 percent at high energies to 65 percent at energies less than 1 Joule. The conditions for the VIS-8 were entered using a remote box that allows the adjustment of energy levels and voltage to achieve the desired ignition energy.

3. Vacuum System

The vacuum system is an integral part in ensuring the mixture being detonated is a known composition. It is made of a solenoid operated vacuum valve at the aft end of the combustor and the vacuum pump itself. A view of the vacuum valve looking towards the head end of the combustor can be seen in Figure [3-3].

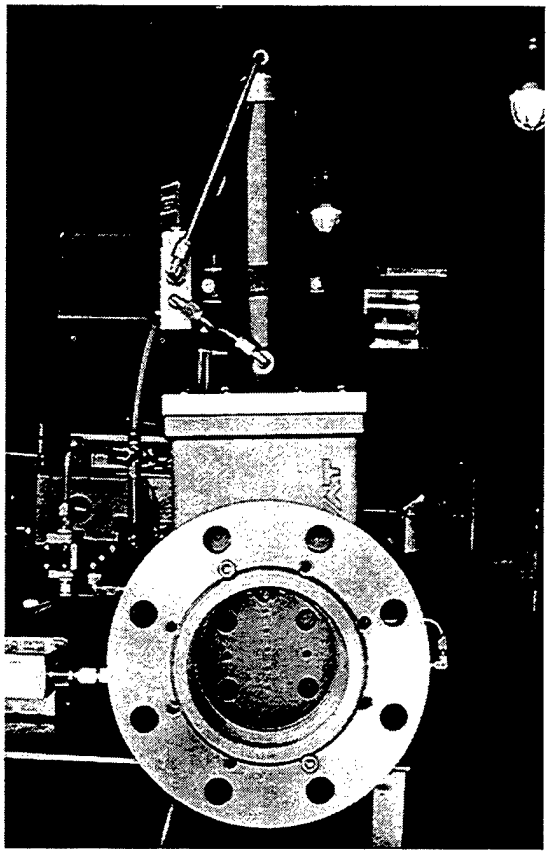

Figure [3-3]. Vacuum Valve in the Closed Position.

The system allows the combustor to be evacuated down to 0.2 psig so that it may be refilled with the desired reactants and equivalence ratio. It also allows the combustor to be isolated from the atmosphere while the reactants are mixing through diffusion over a 10 to 15 minute period. Once the reactants were mixed, the vacuum valve was opened. A micro-switch embedded in the valve closes when the valve is open, thereby enabling the ignition system to be discharged.

4. Fuel Control System

The fuel control system allowed the gases to be delivered to the combustion tube. Since equivalence ratio of the reactants is a controlled variable, the measurement and management of gas flow is a critical factor in the validity of the experimental procedure. It was accomplished through a series of solenoids, ball valves, flow restrictive needle valves and check valves. The experiment calls for two separate pure gases, ethylene and oxygen, and air, therefore two plumbing lines were run in parallel to the combustor. Figure [3-4] is a schematic of the fuel control system.

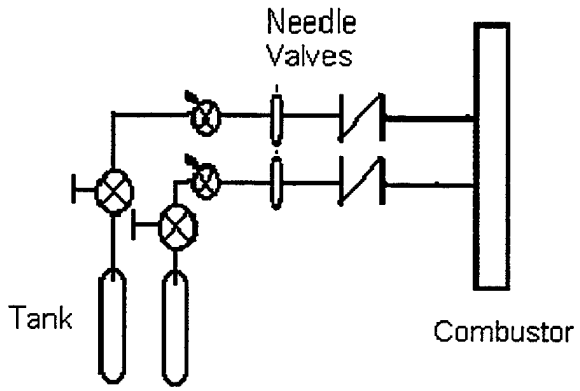

Figure [3-4]. Schematic of Fuel Control System.

The gases were supplied from pressurized gas bottles regulated down to a constant pressure of 100 psig. The combustor was isolated from the gases by nitrogen-actuated ball valves that were opened only during run operations. During the filling process, the specific gas was delivered at a rate which resulted in a chamber pressure fill rate of 0.4 $^{psig}/_{sec}$ through a needle valve into the sidewall of the combustor. Stoichiometry was controlled by monitoring the tube pressure. A check valve provided the safety to prevent backflow of gases or shock waves into the fuel lines. The pressures within the lines and in the combustor were constantly monitored through calibrated transducers.

C. REACTANTS

The reactants chosen for this experiments were chosen due to the ease at which they detonate and the relatively short deflagration to detonation transition (X_{DDT}) distance. The mixtures detonated were various equivalence ratios of ethylene (C_2H_4) and oxygen (O_2) / nitrogen (N_2) blends. The oxygen content of the mixture was then lowered by combining it with air to test the effects of nitrogen dilution on X_{DDT} within the combustor. The mixture was loaded into the combustor starting at 0.3 psi vacuum and filled sequentially until the calculated amount of gas is present. Ethylene was filled first to ensure the maximum amount of natural diffusion could take place under sub-atmospheric pressures. This followed immediately by filling of oxygen until the absolute pressure inside the combustor reached 1.0 atm.

Using partial pressures of the individual reactants, derived from the desired equivalence ratio, the amount of each reactant within the tube could be accurately measured. The following equations were derived for the partial pressure of the reactant for a given equivalence ratio (φ). The equivalence ratio is defined as the ratio of the actual fuel to oxidizer ratio to the stoichiometric fuel to oxidizer ratio. The fuel to oxidizer ratio (*F*/O) can be calculated by dividing the number of moles fuel by the number of moles of oxidizer.

$$\phi = \frac{(F/O)}{(F/O)_{ST}} \qquad [3\text{-}1]$$

Using this definition along with the relationship of partial pressures,

$$\frac{p_i}{p_0} = \frac{n_i}{\sum_{i=1}^{N} n_i} = X_i \qquad [3\text{-}2]$$

where n_i is the number of moles of the gas in the mixture, the required partial pressure of the reactant for a given φ can be determined. For the pure ethylene / oxygen mixture the equation for the fill pressures become,

$$p_{ethyl} = \frac{\varphi}{\varphi + 3} p_0 \qquad [3\text{-}3]$$

$$p_{ox} = \frac{3}{\varphi + 3} p_0 \qquad [3\text{-}4]$$

The experiments investigating N_2 dilution required the use of air within the mixture. The significant percentage and known content of nitrogen (N_2) in air lends itself as a good gas to incorporate into the reduced oxygen mixture. Experiments led to the conclusion that a 75/25% oxygen to nitrogen would be the lowest possible ratio to evaluate and still produce X_{DDT} distances within the combustor tube. Conducting a similar analysis noted above, the fill pressures for the individual gases became,

$$p_{ethyl} = \frac{\varphi}{\varphi + 4} p_0 \qquad [3\text{-}5]$$

$$p_{ox} = \frac{2.734}{\varphi + 4} p_0 \qquad [3\text{-}6]$$

$$p_{air} = \frac{1.266}{\varphi + 4} p_0 \qquad [3\text{-}7]$$

Because the combustor is filled sequentially, the final pressure of the tube is one atmosphere (p_0). The control screen that allows the user to change run conditions within the program is shown in Figure [3-5].

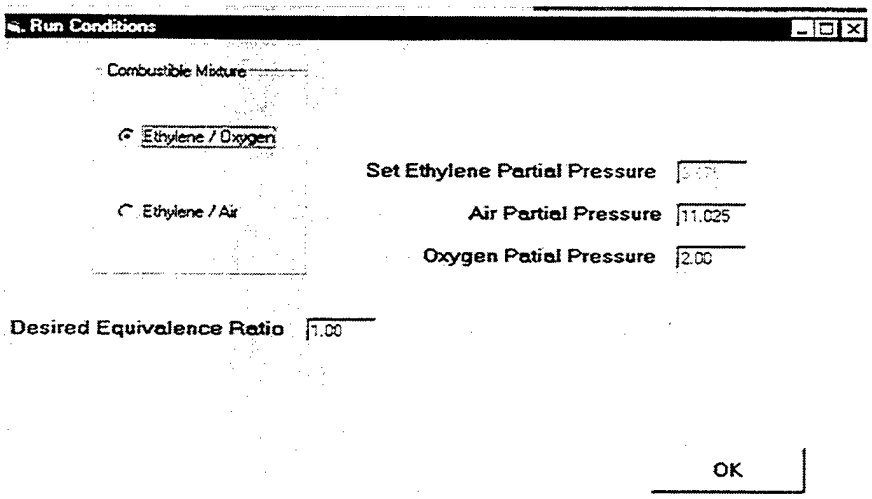

Figure [3-5]. Control Screen for Altering Mixture Ratios. [From Ref. 9]

D. SOFTWARE DESCRIPTION AND FUNCTIONS

The software used for the experimental procedure was designed and written to allow precise control of the gas flow and monitoring of the combustor parameters. It accomplishes this while leaving the human interface open to initiate the ignition or to counter any malfunctions within the system during the test. The control code was designed and written using Microsoft® Visual Basic 5.0 GUI software [Ref. 9]. Initial test parameters, including mixture type and equivalence ratio could be changed prior to each test within a subroutine of the control code shown in Figure [3-5]. The program also allowed for the real-time visual representation of the detonation facility in operation. All valve and ignition commands were executed by TTL signals through a PIO24 board with a bank of Crydom 6321 solid-state relays to the specific component. The control code continually updated the detonation tube pressure and the pressures of the individual reactants to allow a visual check of the facility's status. Imbedded within the program were timing sequences that controlled critical safety measures in firing delays and timing

of the data acquisition sequence. The layout of the facility operation screen can be seen in Figure [3-6].

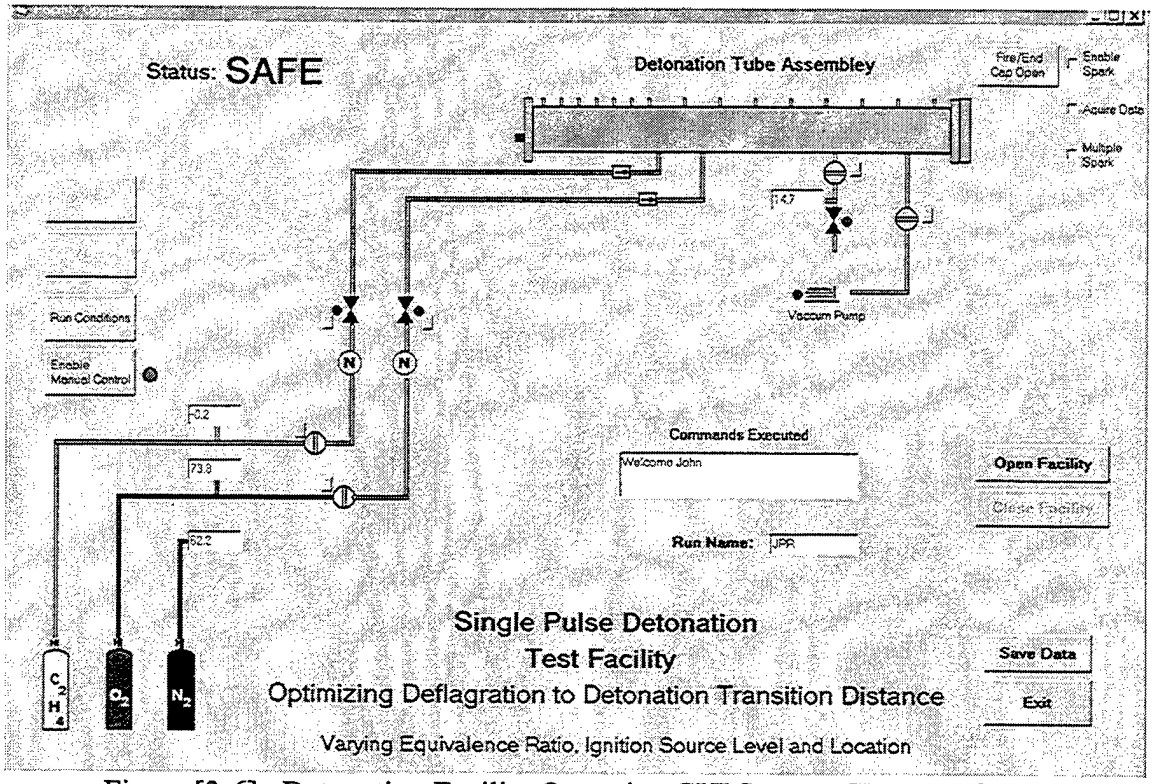

Figure [3-6]. Detonation Facility Operation GUI Screen. [From Ref. 9]

Construction of the facility control code was also useful in gaining a full understanding of the test setup, procedure, data acquisition, and facility control prior to the first experiment.

E. EXPERIMENTAL TEST PROCEDURE

The testing procedure was a sequence of events that allowed for careful control of the experimental parameters while maintaining the physical checks required for the facility's safe operation. In general, the following is a systematic account of the facility's setup, operation and securing for a given experiment:

- Open the facility and set experimental parameters including type of mixture, equivalence ratio, ignition source energy level and ignitor location. Start the run sequence and allow code to complete the following steps.
- Close the vacuum valve and turn on vacuum pump to decrease the tube pressure to 0.3atm.
- Open ethylene fuel valves to the combustor and fill to calculated partial pressure of fuel needed to match the desired equivalence ratio.
- Secure ethylene. Open oxygen lines to combustor and fill it to a pressure of 1atm.
- Isolate the combustor and allow mixture to naturally diffuse inside for 10 minutes.
- Code enables ignitor. Once a safety check on the firing range is cleared, the spark was enabled and the vacuum valve opened.
- The data acquisition board was initiated once the end cap was completely open.
- A micro-switch inside the vacuum valve closes the ignitor loop when it is opened, initiating the detonation with the selected spark energy.
- Upon completion of detonation, data was stored and the facility closed.

The formalized standard operating procedure for the facility's setup, operation and securing for a given test day is included as an Appendix. Careful review of this procedure prior to each day of experimentation allowed for the safe operation and careful control of the testing integrity.

F. DATA GATHERING AND PROCESSING

The only source of data that was utilized to analyze the wave structure of the combustion event was the static pressure of the wave as it passed over given lengths of the combustor as a function of time. Due to the severe pressures, temperatures, and significant wave speeds created by a detonation, the pressure transducers were required to be protected with a silicone coating. Seven Kistler 603B1 pressure transducers which have a frequency response greater than 500 KHz were used to accomplish this. They were amplified through 5010B dual mode charge amplifiers with 540kHz notch filters. Two Microstar Labs 3400a/415 12-bit data acquisition boards recorded the signals generated by the amplifiers. The sample rates of the boards were set to 500 KHz per channel and were synchronized to record all channels simultaneously.

The data acquisition sequence was initiated when the opening vacuum valve closed the ignition loop. The board recorded data for 2.5 seconds before the storage capacity on the data acquisition boards was full. This allowed enough time to capture the detonation wave as it transitioned and traveled out the combustor tube. Figure [3-7] is a plot of the raw data points acquired through a detonation wave in a typical detonation experiment.

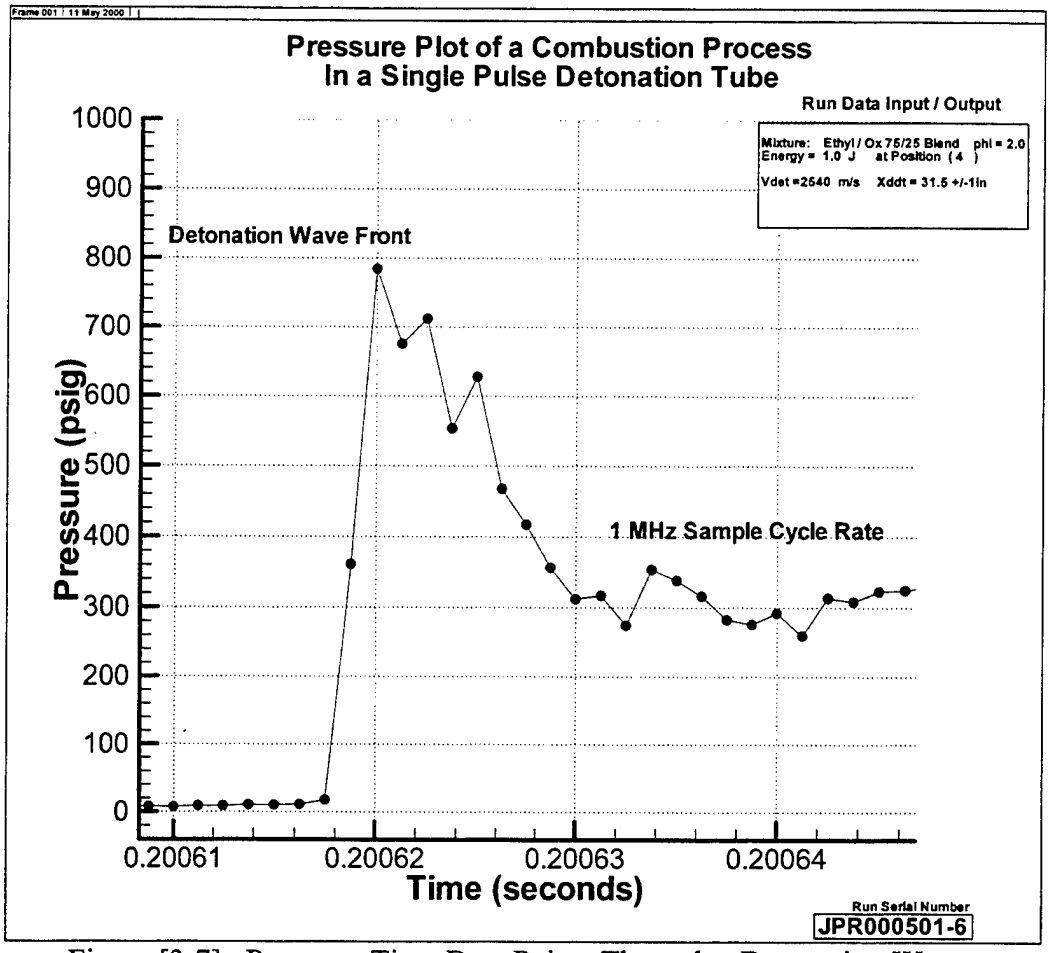

Figure [3-7]. Pressure–Time Data Points Through a Detonation Wave.

Once recorded the pressure-time traces could be analyzed using the graphics software in TecPlot 7.5

G. EXPERIMENTAL TEST MATRIX

The goal of the experiment was to determine how specific changes in the initial conditions of the reactants and ignition source affected the length at which the combustion process transitions from a deflagration to a detonation wave. In order to logically test all parameters being investigated without convoluting their effects, a careful test matrix was developed. This matrix looked at four independent variables, ignition source energy, ignition source location, reactants' equivalence ratio, and reactants' oxygen content. Table [3-1] lists the specific conditions tested for each parameter.

Table [3-1]. Independent Parameters Tested for X_{DDT}.

Variable	Values Investigated	Units
Ignition Energy Level	0.33, 0.5, 0.8, 1.0, 5.0, 8.31	Joules
Equivalence Ratio	0.6, 0.8, 1.0, 1.2, 1.5, 2.0	None
Ignition Source Location	0.0, 3.0, 7.0	Inches from Head Wall
Reactant O_2/N_2 Ratio	100, 75	Percentage

Through combinations of each of these, the deflagration-to-detonation transition (X_{DDT}) distance was determined by analyzing the developing wave's pressure traces. Not all combinations were tested, due to time constraints and little experimental value certain data points would produce. Each experiment was conducted at least once, therefore, little analysis was conducted on the shot-to-shot deviation of the experiments.

THIS PAGE INTENTIONALLY LEFT BLANK

IV. EXPERIMENTAL RESULTS

A. ANALYSIS CRITERIA

The object of these experiments was to determine the deflagration-to-detonation transition (X_{DDT}) distance for various combinations of initial conditions listed in Chapter III.G. A standard set of guidelines was outlined to compare experimental data for X_{DDT} determination. The following is a list of these guidelines and an explanation of why they were positive indications of a detonation transition.

- The wave velocity is greater than 90% of the theoretical detonation velocity. This is the strongest indication that a detonation had fully transitioned. Both theory and experiments show that there exists a 500 to 1200 $^{m}/_{s}$ difference in deflagration driven shock velocities and detonation wave velocities. This criterion in velocity difference is common and has been used in the earliest experiments of detonation waves [Ref. 1].
- The wave's static pressure must exhibit a substantial step increase. The ZND wave structure models the detonation wave with a sharp increase in pressure. This is caused by a normal shock followed immediately by a reaction zone as seen in Figure [2-3]. Experimentally this is seen as a near step increase in the pressure traces of known detonations. This can be seen in Figures [2-8], [2-9], [2-11] and [3-4], and proves to be a strong indication of a detonation wave.

If both of these criteria were met, the wave was considered fully transitioned at that transducer location. The X_{DDT} distance was then deemed to occur midway between that

transducer and the previous transducer. The margin of error on the X_{DDT} distance determination is the distance between transducers.

B. COMPLETED EXPERIMENTAL TEST MATRICES

1. Ethylene / Oxygen with Ignitor at Head Wall

The goal of the first experimental test matrix was to complete a detailed plot of the effects of varying ignition energy level and mixture equivalence ratio on X_{DDT} distance. The simplest conditions were set to ensure a detonation within the test combustor and gain experience with the gaseous mixture. The reactants used were ethylene and oxygen, which are known to have X_{DDT} distances of less than 12 inches near stoichiometric conditions. The second condition evaluated was the ignition source location. The ignitor was placed on the head wall to minimize any effects of multiple combustion fronts or shock focusing. Pressure transducers were placed two inches apart, to ensure capturing estimated X_{DDT} distance. Once successful operation of the test facility was confirmed and the initial course test matrix completed, the test procedure outlined in Chapter III.E and the Appendix was initiated.

The test matrix covered a range of ignition energies from 0.3 to 8.0 Joules over several mixture equivalence ratios from 0.8 to 2.0. The ignition energy range was based on the limits of the ignition system. The equivalence ratio parameter range was based on the detonability limits found experimentally and discussed in Chapter III.E.2. The results of this experimental matrix are recorded in Table [4-1].

Table [4-1]. Ethylene / Oxygen Test Matrix for Ignitor Position on Head Wall.

Equivalence Ratio ϕ	Energy Level Supplied to Ignitor (Joules)					
X_{DDT}	0.3	0.5	0.75	1.0	2.5	8.0
0.8	8	8	8	8	**X**	8
1.0	6	6	5	5	5	5
1.2	3	3	3	3	3	3
1.5	3	3	3	3	3	3
2.0	6	6	5	5	5	5

The data point at a ϕ of 0.8 and ignition energy of 2.5 was not taken, however the point is not at an inflection and there is no reason to believe the trend would be upset. Each data point was only sampled once; therefore, no statistical results can be made.

Graphically, this data can be presented in two separate ways. The first is an inverted carpet plot, Figure [4-1], that displays how X_{DDT} varies with the initial mixture and spark energy conditions. The optimal conditions are also pointed out at an equivalence ratio of 1.3 and spark energy of 0.3 Joules.

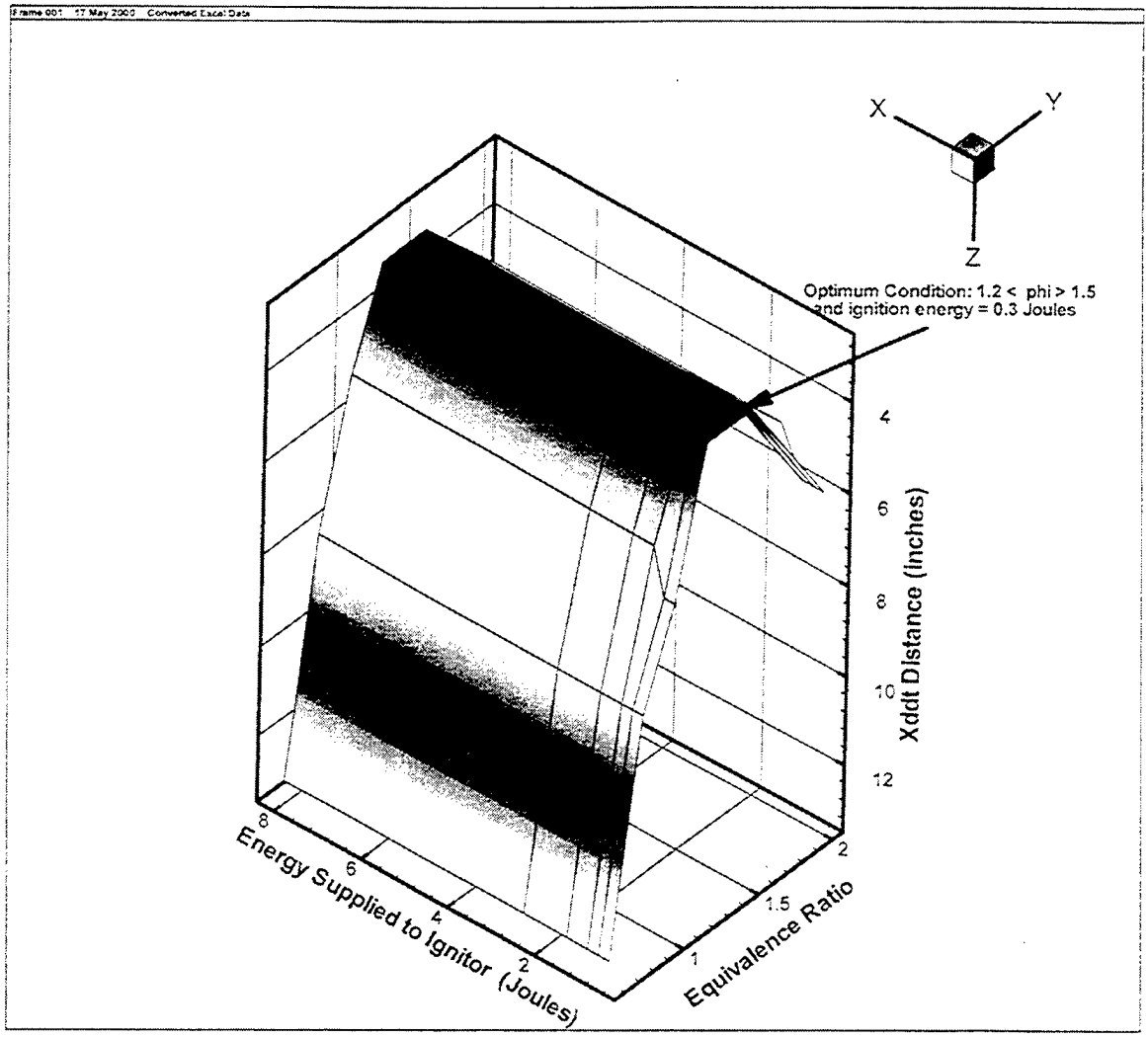

Figure [4-1]. Carpet Plot of Ethylene / Oxygen Baseline Variables Test.

The second way to present the data is a contour plot of X_{DDT} as a function of the reactant equivalence ratio and ignition energy. In the plot, depicted in Figure [4-2], the contour levels are the transition distances for the corresponding ignition energy and equivalence ratio. The light color region shows the optimal conditions to minimize X_{DDT} and required ignition energy.

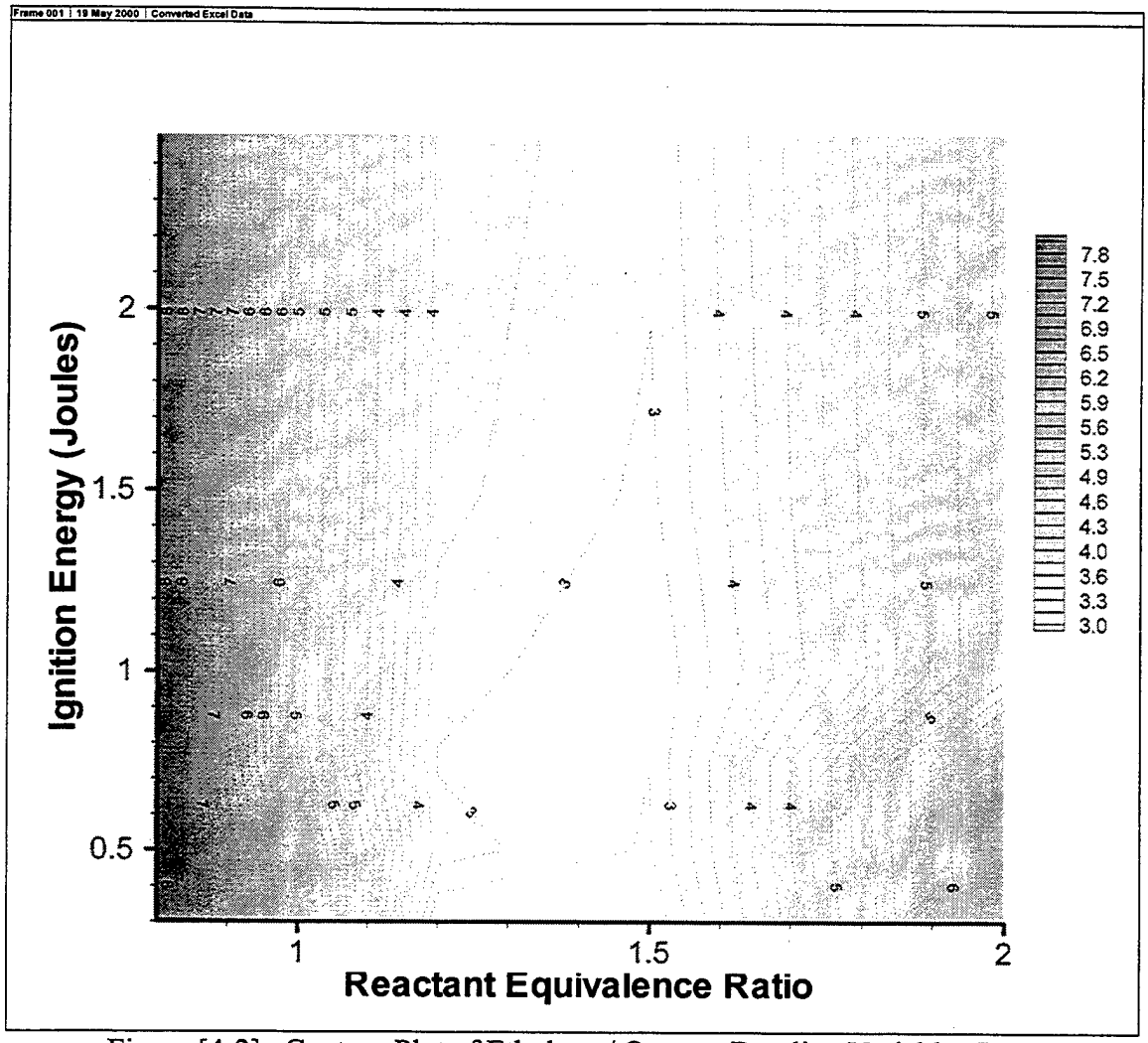

Figure [4-2]. Contour Plot of Ethylene / Oxygen Baseline Variables Test.

Analysis of the results of the experimental test matrix will be discussed in Sections C and D of this chapter.

2. Ethylene / Oxygen-Nitrogen Blend with Ignitor at Head Wall

The goal of this test matrix was to sample the effects of lowering the oxygen content of the oxidizer, through N_2 dilution, on X_{DDT} distance. The ignition level and mixture equivalence ratio range were duplicated and compared with the first test matrix. The ignitor was left on the head wall of the combustor.

The test matrix covered the same range of ignition energies and mixture equivalence ratios as the ethylene/oxygen test matrix. The results of this experimental matrix are recorded in Table [4-2].

Table [4-2]. Ethylene / Oxygen-Nitrogen Blend Test Matrix for Ignitor Position on Head Wall.

Equivalence Ratio ϕ	Energy Level Supplied to Ignitor (Joules)				
	X_{DDT}	0.33	0.5	1.0	8.31
	0.6	Outside tube	Outside tube	Outside tube	Outside tube
	0.8	16	14	12	14
	1.0	16	12	12	10
	1.2	16	12	12	12
	2.0	20	20	18	18

X_{DDT} transition distances could not be determined for tests conducted at a ϕ of 0.6. Pressure traces showed that a strong shock wave was forming, but wave velocities at the end of the tube were not yet equal to that of a detonation.

The contour plot presents the results in the best manner. The optimal conditions are pointed out at an equivalence ratio of 1.1 and spark energy of 0.5 Joules. Figure [4-3] is a graphical representation of the contour plot.

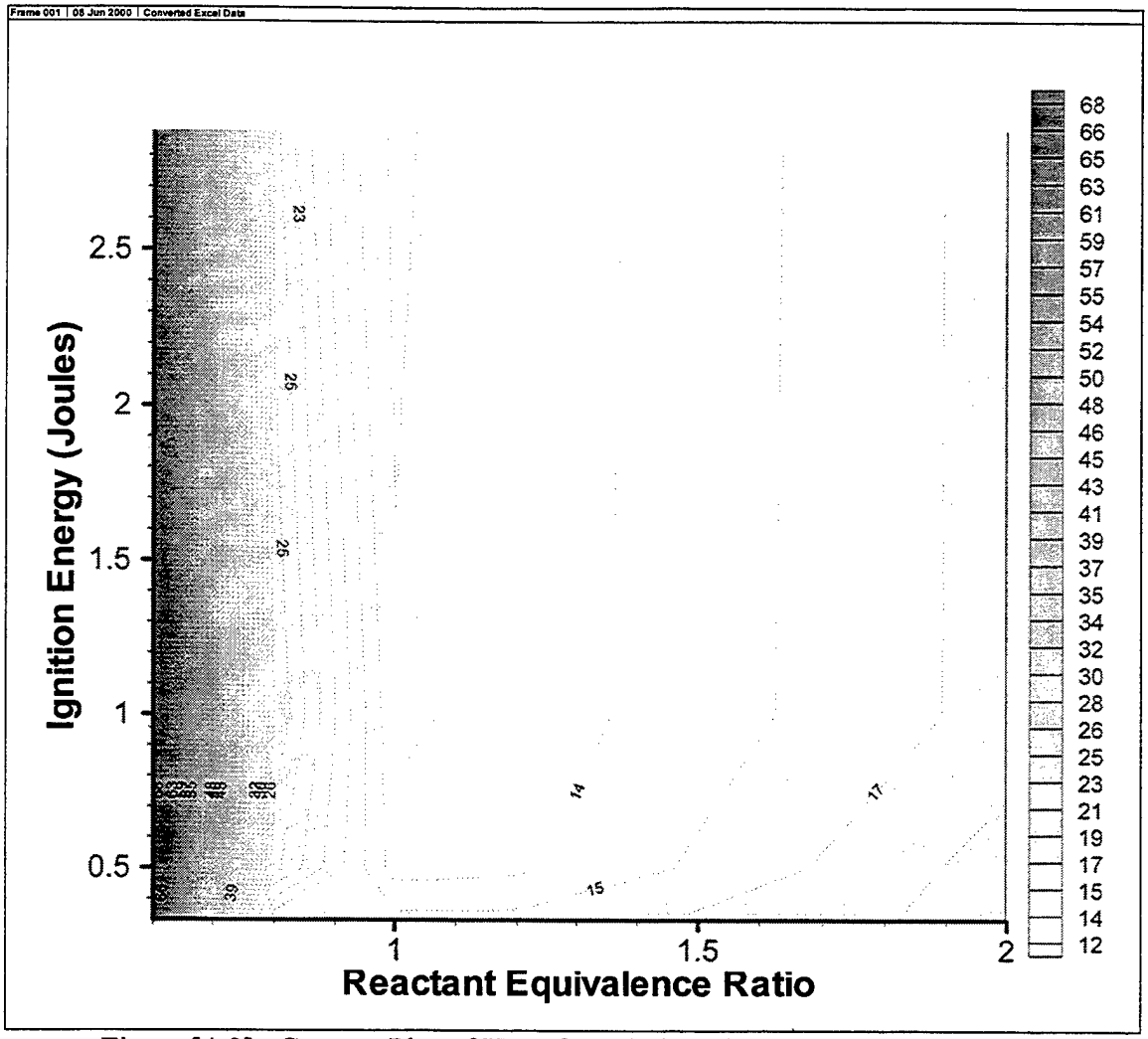

Figure [4-3]. Contour Plot of X_{DDT} for Ethylene / Oxygen-Nitrogen Blend with Ignitor Located on the Head Wall.

3. Ethylene / Oxygen-Nitrogen Blend with Ignitor 3" from Head Wall

The goal of this test matrix was to determine the effects of relocating the ignitor on X_{DDT} distance. The ignitor was placed one tube diameter, 3", from the head wall to determine the benifits of creating two reaction fronts, thereby doubling the inital energy release rate and shorten the X_{DDT} distance. The ignition level and mixture equivalence ratio were again the variables varied with the test matrix outlined in Section B.2 of this chapter.

The test matrix covers the same range of ignition energies and mixture equivalence ratios as in the previous experiments. The results of this experimental matrix are recorded in Table [4-3].

Table [4-3]. Ethylene / Oxygen-Nitrogen Blend Test Matrix for Ignitor 3" from Head Wall.

Equivalence Ratio ϕ	Energy Level Supplied to Ignitor (Joules)				
	X_{DDT}	0.33	0.5	1.0	8.31
	0.6	39	33.5	33.5	33.5
	0.8	12	12	10	10
	1.0	12	10	8	8
	1.2	12	12	12	12
	2.0	20	18	16	16

The contour plot of the results is shown in Figure [4-4]. The optimal conditions shown at the start of the light region are at an equivalence ratio of 1.0 and spark energy of 1.0 Joules.

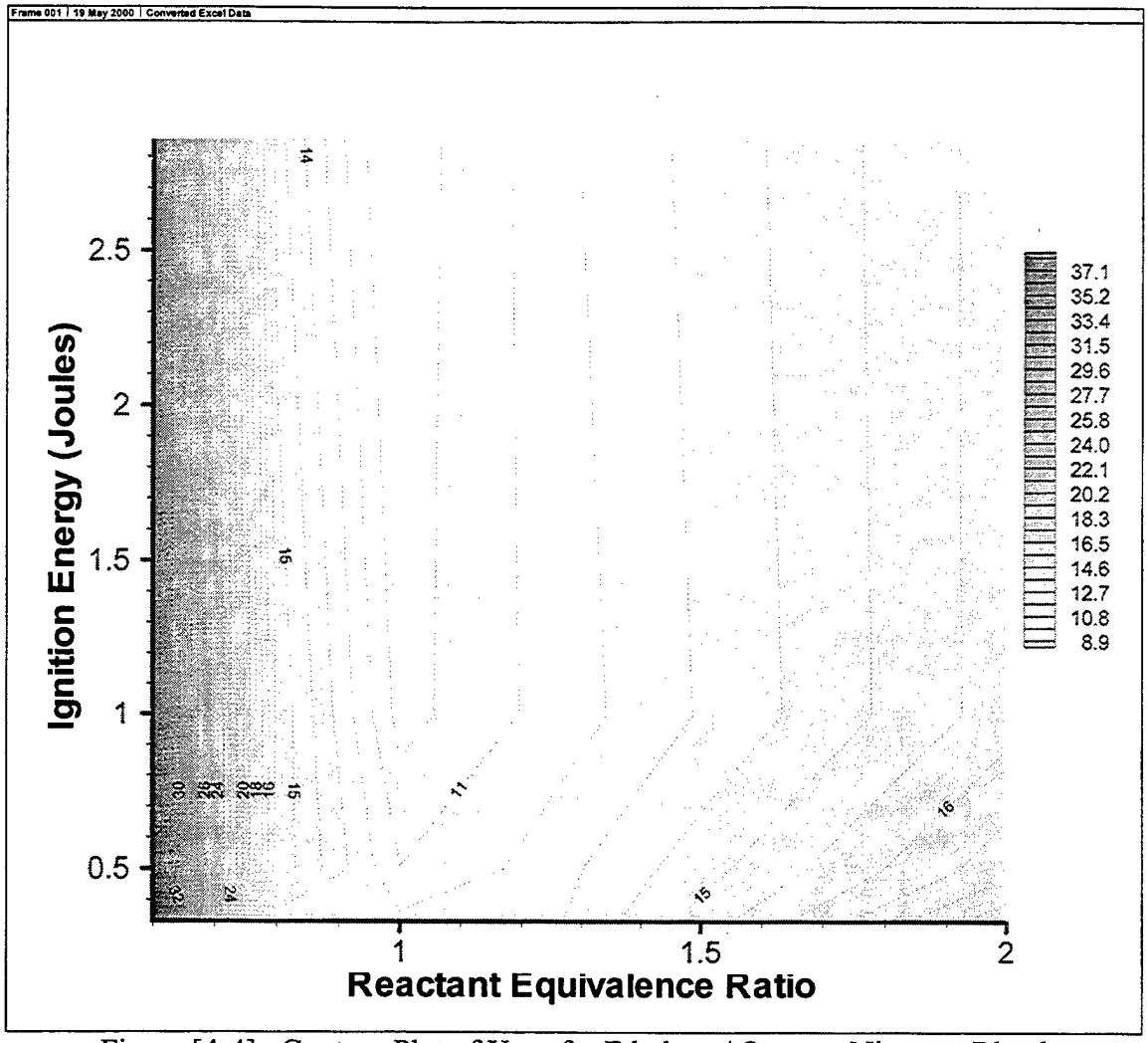

Figure [4-4]. Contour Plot of X_{DDT} for Ethylene / Oxygen-Nitrogen Blend with Ignitor Located 3" from the Head Wall.

4. Ethylene / Oxygen-Nitrogen Blend with Ignitor 7" from Head Wall

The goal of the last test matrix was to continue to evaluate the effects of relocating the ignitor on X_{DDT} distance. The ignitor was placed approximately two tube diameters, 7", from the head wall to determine if there exists any further benefits in minimizing X_{DDT}. The ignition level and mixture equivalence ratio were again varied as described in Section B.2 and B.3 of this chapter.

The test matrix covers the same range of ignition energies and mixture equivalence ratios as in the previous experiments. The results of this experimental setup are recorded in Table [4-4].

Table [4-4]. Ethylene / Oxygen-Nitrogen Blend
Test Matrix for Ignitor 7"from Head Wall.

Equivalence Ratio ϕ	Energy Level Supplied to Ignitor (Joules)				
	X_{DDT}	0.33	0.5	1.0	8.31
	0.6	Outside tube	Outside tube	Outside tube	Outside tube
	0.8	20	18	18	16
	1.0	18	16	16	16
	1.2	20	18	18	18
	2.0	31.5	31.5	31.5	31.5

The contour plot is shown in Figure [4-5] depicts the data contained in Table [4-4]. The optimal conditions are shown to be at an equivalence ratio of 1.0 and spark energy of 0.5 Joules.

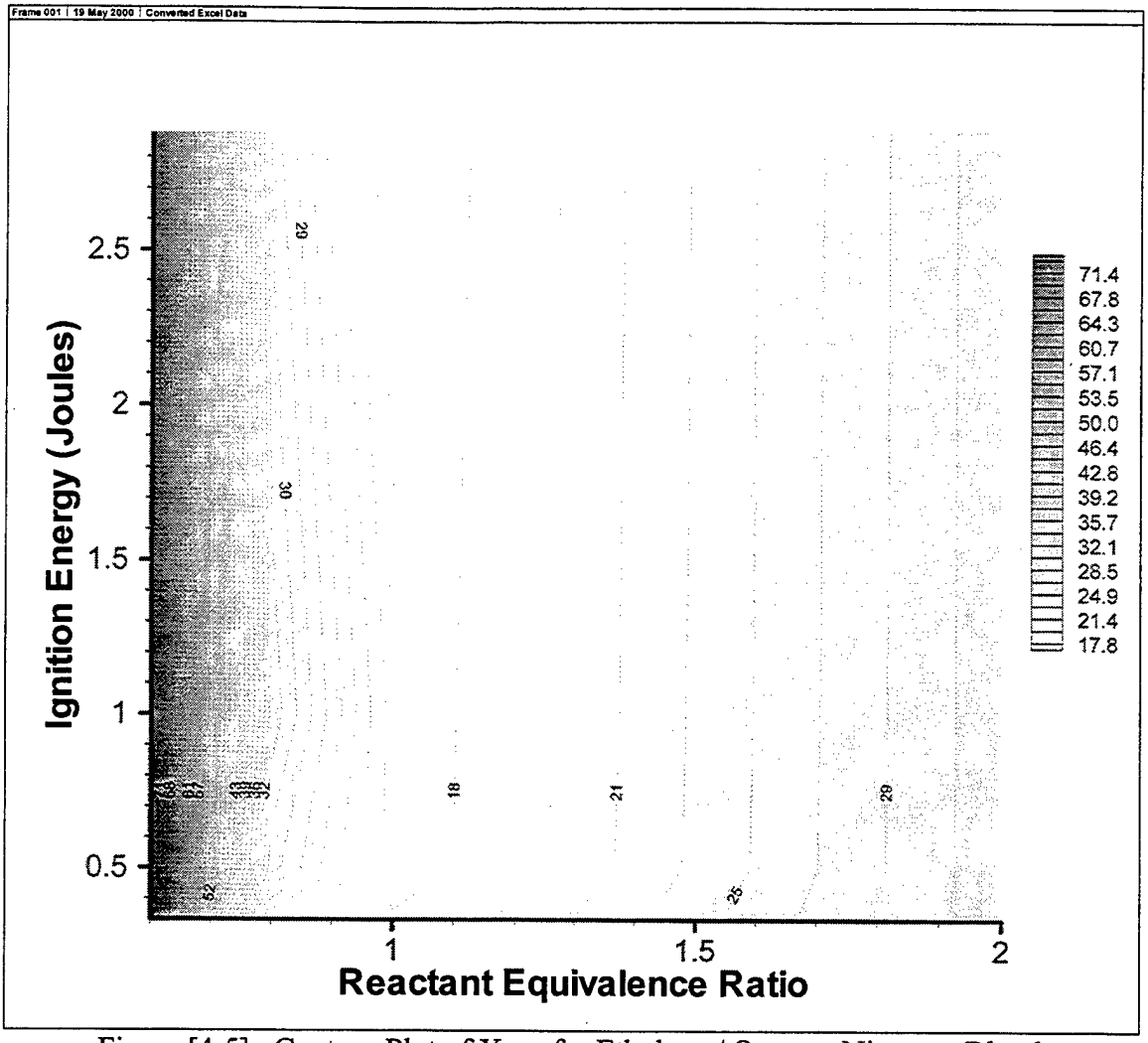

Figure [4-5]. Contour Plot of X_{DDT} for Ethylene / Oxygen-Nitrogen Blend with Ignitor Located 7" from the Head Wall.

5. Uncertainty Analysis

There are inherent errors in the measurements taken for these experiments due to the nature of the parameters being measured. Specifically, the two values that are of interest in the uncertainty calculations are in the detonation velocity (V_{det}) and the deflagration-to-detonation transition distance. Two parameters that are critical in making judgments on the detonation wave structure and transition characteristics.

The detonation velocity, V_{det}, was calculated by analyzing the pressure-time trace and applying the rate equation to the passing detonation wave. This analysis is detailed

in Chapter II.E.2. The error in this calculation stems from the two variables in equation [4-1]. The error in Δx is due to the physical errors of pressure ports in the combustor.

$$V_{det} = \frac{\Delta x}{\Delta t} \qquad [4\text{-}1]$$

Tolerance specifications on these ports were 0.005 inches from centerline, which corresponds to a total distance error between test ports of $\Delta x = \pm$ 0.01 inch. The second source of uncertainty arises from the sample rate of the data acquisition board. The board samples at a 500 KHz frequency, therefore the pressure wave may hit the transducer in between data samples. The time error in the rate equation becomes $\pm 0.50 \times 10^{-6}$ seconds. Knowing these sources of error, the detonation velocity uncertainty can be calculated including error terms from the experiments.

The error in determining X_{DDT} is not as definitive as the velocity's error term due to the required interpretation of the developing wave structure. This technique is described in detail in Chapter II.E.1. The error in determining X_{DDT} is derived from the distance between the pressure transducers. The transitioning wave may not have been developed at one test port, but at the next show a fully transitioned wave. Therefore, the actual transition occurred between the two transducers. The error in this determination becomes the actual distance between the two transducers where the transition occurred. This was not a precise measurement with errors on the order of one or two inches due to human interpretation of the pressure traces. However trends can be developed with these measurements describing the effects of changing initial parameters on X_{DDT}

C. EFFECTS OF EQUIVALENCE RATIO ON X_{DDT}

The detonable mixture's equivalence ratio was an important factor in how rapidly it was able to transition into a detonation. This was expected since most of the energy released during the event comes from the chemistry of combustion. To analyze the specific effect of altering the equivalence ratio of the reactants, a breakdown of the contour plots into a two-dimensional X-Y plot is provided. By holding all other variables constant, a good indication of the strong influence the mixture equivalence ratio has on a transitioning detonation can be seen. The following figures, Figure [4-6], [4-7], and [4-8], represent each of the three ignitor locations. Each plot displays the four different ignition energies tested for the specific ignition location. Five different equivalence ratios of the ethylene / oxygen-nitrogen blend were tested and presented.

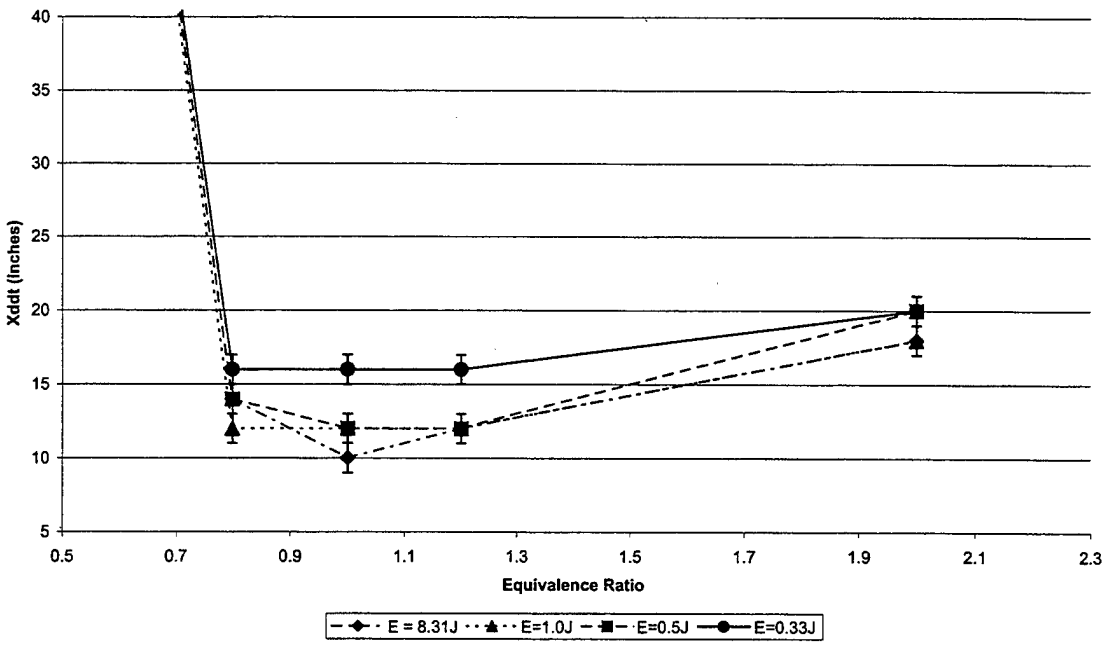

Figure [4-6]. X_{DDT} Distance as Function of Equivalence Ratio with Head Wall Ignition.

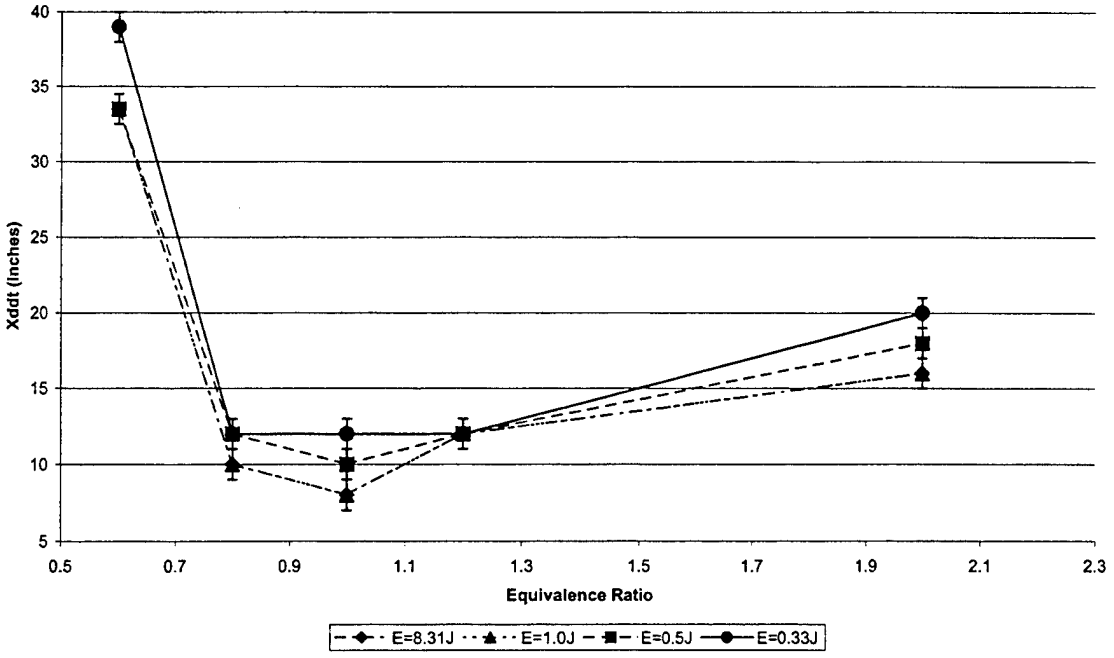

Figure [4-7]. X_{DDT} Distance as Function of Equivalence Ratio with Ignition 3" from Head Wall.

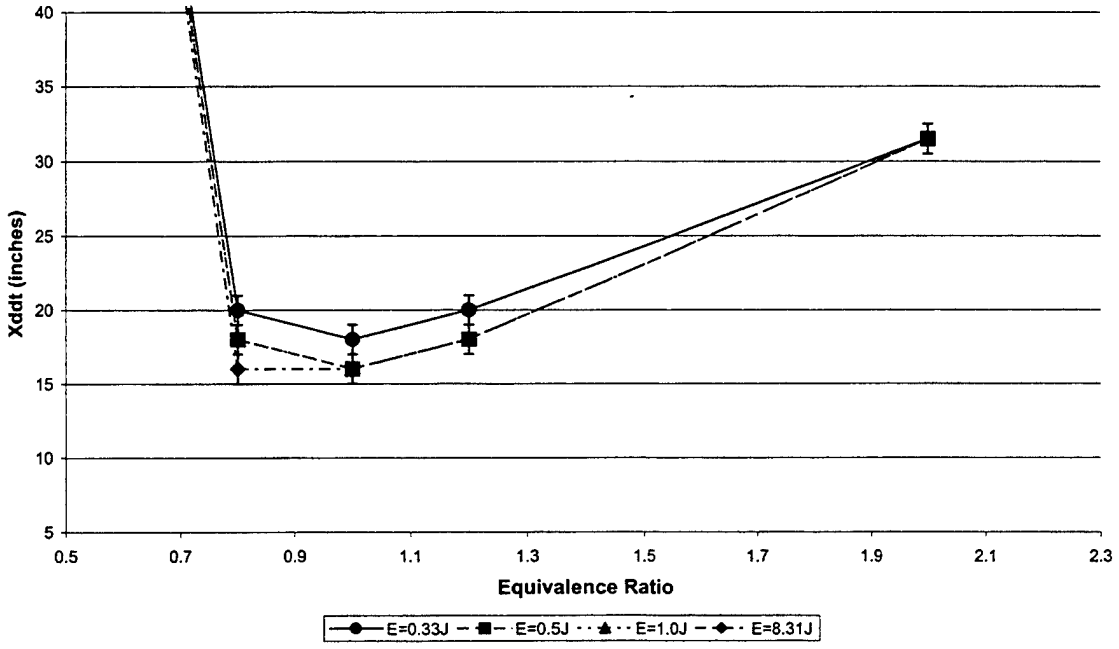

Figure [4-8]. X_{DDT} Distance as Function of Equivalence Ratio with Ignition 7" from Head Wall.

It can be seen in these plots that the optimized equivalence ratio for every condition lies from a range of φ's from 0.9 to 1.2. In addition, there is a sharp increase in X_{DDT} for φ's less than 0.75. In contrast, there was a much more gradual increase in X_{DDT} for higher equivalence ratios. In a practical system, the data supports the running a Pulse Detonation Engine with this specific mixture at equivalence ratios slightly greater than stoichiometric. This would minimize the detonation transition distance while also allowing for fuel load variations without substantially impacting the engine's cycle. These results produce a repeatable trend in the behavior of a transitioning detonation wave varying mixture equivalence ratios.

D. EFFECTS OF IGNITION ENERGY ON X_{DDT}

Ignition energy was investigated to determine the minimum energy required to initiate a detonation in the shortest distance. The X_{DDT} distance was expected to be minimized at high ignition energies due to the amount of energy initially supplied to the reactants. A series of two-dimensional figures show the effects of ignition energy on a transitioning detonation for the three geometries investigated. The following figures, Figure [4-9], [4-10], and [4-11], represent each of the three ignitor locations. Each plot displays the five different equivalence ratios tested for the specific ignition location. Four different ignition energies supplied to the ethylene / oxygen-nitrogen blend were tested and plotted. Ignition energies of 2.0 and 5.0 Joules were also tested and showed no difference in XDDT. For this reason, data points between 1.0 and 8.31 Joules were not shown as they had little influence on the final results.

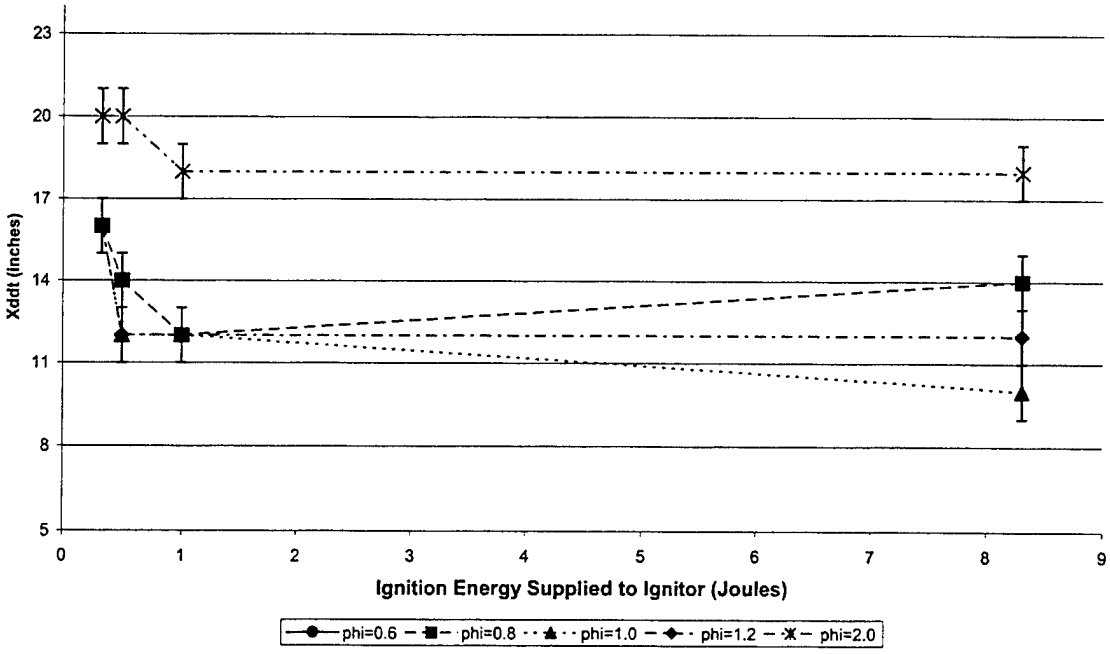

Figure [4-9]. X_{DDT} Distance as Function of Ignition Energy with Head Wall Ignition.

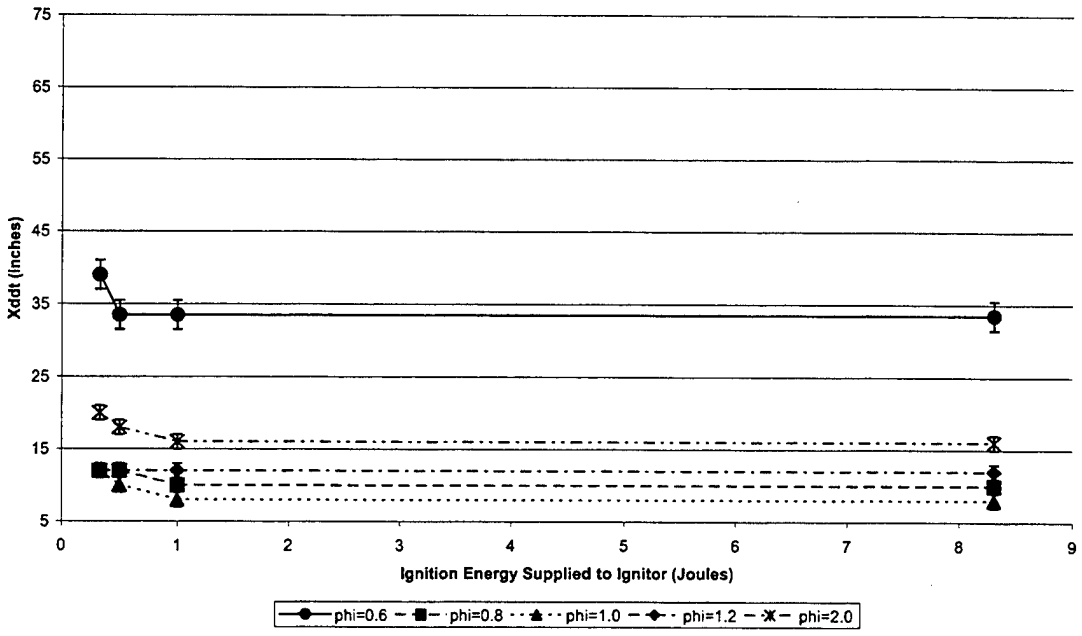

Figure [4-10]. X_{DDT} Distance as Function of Ignition Energy with Ignition 3" from Head Wall.

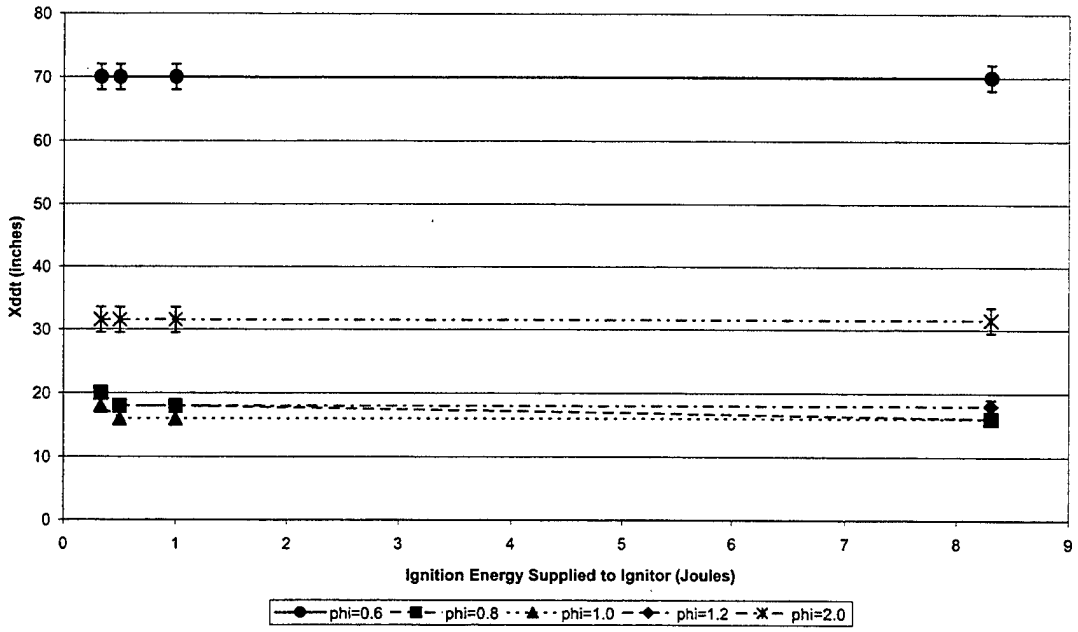

Figure [4-11]. X_{DDT} Distance as Function of Ignition Energy with Ignition 7" from Head Wall.

The data presented in the above figures support the fact that there is little to no dependence on ignition energies greater than 0.5 Joules on X_{DDT}. At energy levels lower than 0.5 Joules the transition distance begins to increase showing that, there is a minimum ignition energy requirement to maintain a minimum X_{DDT} in the initiation of a detonation. This result was a common result throughout all tested conditions.

E. EFFECTS OF IGNITION SOURCE LOCATION ON X_{DDT}

Three separate ignition locations were tested to determine if there exists a way to increase the energy release rate of the reactants in order to shorten the deflagration-to detonation transition distance. The first tests were completed with the ignitor placed at the head wall of the combustor. The following two test matrices were tested at ignition locations one and two combustor tube diameters from the head wall. Reviewing the data presented in Tables [4-2], [4-3], and [4-4], it is clear that there was some influence of ignition location on X_{DDT}. The average value of the minimized X_{DDT} for head wall

ignition taken from Table [4-2] is 12.5 inches. The average value of the minimized X_{DDT} for the ignition located one tube diameter from the head wall, taken from Table [4-3], is 9.5 inches. The average value of the minimized X_{DDT} for the ignition located two tube diameters from the head wall, taken from Table [4-4], is 16.5 inches.

It is clear that by placing the ignitor one tube diameter from the head wall reduced the X_{DDT} by 24%. However, there is a limit to how far you can move the ignitor from the head wall. By placing the ignitor two tube diameters from the head wall, the X_{DDT} was increased by 24%. This result shows the advantage to locating the ignition source to a position that amplifies the energy release rate of the reactants just after ignition. Future testing could explore this phenomenon by altering ignition strategies to further reduce the deflagration-to detonation transition distance.

F. EFFECTS OF DECREASED OXYGEN CONTENT ON X_{DDT}

In order to understand the effects of N_2 dilution in the oxidizer, four separate mixtures of ethylene (C_2H_4), oxygen (O_2), and nitrogen (N_2) were tested to determine the effect on X_{DDT}. Since an air-breathing propulsion system should utilize as much air for the oxidizer as possible, the pure oxygen carried on board must be minimized for volume, safety, and performance considerations. The four mixtures tested were various percentages of oxygen and nitrogen that make up 75% of the total mixture. Ethylene was the fuel used for all the tests. The first test mixture was made up of pure oxygen with no nitrogen present. The second test attempted to use air (24% oxygen to 76% nitrogen). The third and fourth test used a 50%/50% and 25%/75% oxygen/nitrogen blends respectively. Using these parameters, the effect of varying the nitrogen content in the mixture could be investigated.

The gaseous mixture with no nitrogen dilution, only ethylene and oxygen, produced the shortest X_{DDT}, as expected. Averaging the minimized distances from Table [4-1], the tests show an average X_{DDT} of 3 inches. Tests using ethylene and air and the 50%/50% oxygen/nitrogen blend were unsuccessful in producing a detonation within the combustor tube. It can be deduced from these failures that if the mixture was detonable, the transition distance is greater than 75 inches and not likely practical for the pre-detonator component of a propulsion system. The fourth and final oxidizer ratio of 75%/25% oxygen/nitrogen was tested and detonated within the combustor tube. Averaging the minimized distances from Table [4-2], the tests show an average X_{DDT} of 12.5 inches. These results show a substantial and detrimental effect of adding an inert gas to the mixture on its detonation characteristics. Although not unexpected, they do show the need for alternate tube geometries and ignition strategies to further minimize X_{DDT} in an air-breathing Pulse Detonation Engine.

THIS PAGE INTENTIONALLY LEFT BLANK

V. CONCLUSIONS

Pulse detonation technology is theoretically a viable propulsion concept with a higher thermal efficiency and simpler combustor design. Utilizing detonations for an air-breathing propulsion system requires a comprehensive research effort that is currently being conducted throughout the aerospace propulsion industry and by the Office of Naval Research. Pulse detonation technology must mature beginning with research in the fundamental behavior of practically developing a detonation wave reliably, many times a second. This thesis investigated fundamental issues by exploring the effects of ignition location, ignition energy, and reactant mixture ratios to minimize the deflagration-to-detonation transition distance of a single detonation wave. The test program revealed, clear trends and demonstrated the effects of these parameters.

The equivalence ratio of the ethylene/oxygen/nitrogen blends was the most important variable since the mixture makeup delivers nearly all of the energy release to sustain the detonation. It was found that the optimized equivalence ratio for nearly all condition range from φ's $\approx$ 0.9 to 1.2. There existed a sharp increase in X_{DDT} for φ's less than 0.75, while proving less significant increases for higher equivalence ratios. In a practical system, the data supports the running a Pulse Detonation Engine with mixtures at equivalence ratios that are slightly fuel rich.

The effects of ignition energy and ignition location on X_{DDT} were conducted to explore the minimum ignition requirements to initiate a detonation in a reasonable distance. The ignition energy supplied to the ignitor was independently varied from 0.33 to 8.31 Joules and revealed that ignition energies above 0.5 Joules had little to no affect

on X_{DDT}. Only for values below 0.5 Joules did the transition distance begin to increase. This indicates that large power requirements for the ignition system in a Pulse Detonation Engine are not required.

The second part of this thesis investigated ignition locations and revealed that when the ignitor is strategically placed one tube diameter from the head wall, the transition distance could be furthered reduced. These results lead to the conclusion that a Pulse Detonation Engine operating with the tested reactants could be initiated from energy levels on the order of standard automobile spark plugs.

The third and final goal of this thesis was to determine the effect of lowering the oxygen content of the reactant on X_{DDT}. The purpose of this investigation was to determine the oxygen content required to develop a detonation in a reasonable combustor length through the deflagration-to-detonation transition process. Four mixtures were used with various percentages of oxygen and nitrogen that make up the oxidizer in the reactants. It was found that for the given combustor length of 75 inches, the minimum oxygen to nitrogen ratio was 75%. This result reveals the sensitivity of detonation initiation in fuel/air mixtures and must be further studied to understand techniques which may be used to accelerate the process on an actual PDE.

This research bounds some of the fundamental limitations on the initiation of a detonation in ethylene/oxygen/nitrogen gaseous mixtures. Though not immediately practical for real-world applications, this fundamental work will aid in future designs of pre-detonators for larger complex Pulse Detonation Engines.

APPENDIX. DETONATOR TEST FACILITY OPERATING PROCEDURE

Standard Operating Procedure (SOP)

Facility Open Procedure

1) Verify "Emergency Shutdown" switch is pushed IN.
2) Turn on 110VAC power supply switch in black wall mounted cabinet.
3) Turn on yellow "compressed gas present" warning lights.
4) OPEN C_2H_4 and O_2 isolation ball valves.
5) Verify vacuum line isolation ball valve is OPEN.
6) Turn on Kistler electronics and set to proper gain and set to OPERATE mode.
7) Turn on video cameras, and other data recording as required by experiment.
8) Open all gas bottles (actuator N_2, Ethylene C_2H_4 and O_2) and set gas supply pressures in bottle room to: $P_{N2} > 75$ psig, $P_{C2H4} \cong 90$ psig and $P_{O2} \cong 90$ psig.
9) Turn on "Boomer" computer and enter into DETONATION Visual Basic control program.
10) In the program, enter the FACILITY OPERATION form.

Run Mode

11) Verify "Emergency Shutdown" switch to the OUT position.
12) OPEN the facility.
13) Wait for 3 minutes or more for tube to vent any combustible mixture.
14) Reboot ignition system and verify it displays default settings.
15) Verify all igniter, solenoid control, and pressure transducer lines are secure.
16) Set desired ignition levels on Remote Ignitor Box.
17) Set RUN CONDITIONS and ignitor energy level within the program.
18) Change FILE NAME to appropriate serial number to save data.
19) Cycle End Cap and verify ignitor sparks
20) Notify Lab personnel that "Single Pulse Detonation Run is about to commence". Ensure all personnel return to the Control Room.
21) Ensure VHS tapes are VCRs. Start Facility VCR and set to RECORD.

********** WARNING **********

The next step will commence the run sequence.
To STOP the run, depress the ABORT pushbutton in the program.

22) Depress START RUN. Wait for gas mixing countdown.
23) 30 seconds prior to detonation, check for golfers on video monitors.
24) When golfers are clear, turn on sirens.
25) Start Line VCR and set to RECORD.
26) Enable SPARK.
27) Press FIRE / ENDCAP Control pushbutton.
28) Depress the SAVE DATA pushbutton
29) Turn off sirens.
30) STOP VCR recording.
31) Upon completion of data collection, CLOSE the facility.

Securing the Facility

1) Depress "Emergency Shutdown" switch and verify it is pushed IN.
2) Exit DETONATION Visual Basic control program.
3) Turn off power to ignition system.
4) Turn off 110VAC panel switch.
5) Secure N_2, C_2H_4 and O_2 gas bottles. Turn OFF "Compressed Gas Present" warning lights.
6) Close C_2H_4 and O_2 isolation ball valves.
7) Turn off Kistler electronics, cameras and VCR.
8) Close door to test cell #1.

THIS PAGE INTENTIONALLY LEFT BLANK

LIST OF REFERENCES

1. Bauer, P.A., Dabora, E.K., Manson, N., "Chronology of Early Research on Detonation Wave", Dynamics of Detonations and Explosions: Detonations Vol 133, AIAA Inc., pp.3-18.
2. Kuo, K.K., *Principles of Combustion*, John Wiley & Sons, Inc., 1986.
3. Forster, D.L., *Evaluation of a Liquid-Fueled Pulse Detonation Engine Combustor*, Master's Thesis, Naval Postgraduate School, Monterey, California, December 1998.
4. Bussing, T., Pappas, G., "An Introduction to Pulse Detonation Engines", AIAA 94-0263, AIAA Inc. January 1994.
5. Adroit System Incorporated, http://www.adroitnet.com/patents.
6. Office of Naval Research, "ONR Pulse Detonation Research Roadmap", Power Point Presentation, June 1998.
7. Van Wylen, G.J., Sonntag, R.E., *Fundementals of Classical Thermodynamics*, Third Edition, John Wiley & Sons, Inc., 1985.
8. *TEP*^{R} for Windows - A Combustion Analysis Tool, Version 1.0, Software Engineering Associates, Inc., Carson City, Nevada.
9. *Visual Basic 5.0* for Windows, Version 5.0, Microsoft®, Bellview, Washington.

THIS PAGE INTENTIONALLY LEFT BLANK

INITIAL DISTRIBUTION LIST

1. Defense Technical Information Center 2
   8725 John J. Kingman Rd., STE 0944
   Ft. Belvoir, VA 22060-6218

2. Dudley Knox Library Center 2
   Naval Postgraduate School
   411 Dyer Rd.
   Monterey, CA 93943-5101

3. LT John P. Robinson 2
   P.O. Box 345
   Wetumpka, AL 36092

4. Dr. Christopher M. Brophy, Code AA/Br 2
   Department of Aeronautics and Astronautics
   Naval Postgraduate School
   Monterey, CA 93943-5000

5. Dr. David W. Netzer, Code AA/Nt 2
   Department of Aeronautics and Astronautics
   Naval Postgraduate School
   Monterey, CA 93943-5000

6. Dr. Gabriel Roy 1
   Office of Naval Research
   Mechanics Division, Office 333
   Ballston Tower One
   800 N. Quincy Street
   Arlington, VA 22217-5660

7. William B. Maier, Code PH/Mw 2
   Physics Department
   Naval Postgraduate School
   Monterey, CA 93943-5000

8. Tom J. Hofler, Code PH/Ht 1
   Physics Department
   Naval Postgraduate School
   Monterey, CA 93943-5000

9. Curriculum Office, Code 34 1
   Mechanical Engineering Department
   Naval Postgraduate School
   Monterey, CA 93943-5000